



# Vasorelaxant Activities and its Underlying Mechanisms of Magnolia Volatile Oil on Rat Thoracic Aorta Based on Network Pharmacology

Jin-Feng Xu<sup>1</sup>, Jia Xia<sup>1</sup>, Yan Wan<sup>1</sup>, Yu Yang<sup>1</sup>, Jiao-Jiao Wu<sup>1</sup>, Cheng Peng<sup>1\*</sup> and Hui Ao<sup>1,2\*</sup>

<sup>1</sup>Key Laboratory of Southwestern Chinese Medicine Resources, Chengdu University of Traditional Chinese Medicine, Chengdu, China, <sup>2</sup>Innovative Institute of Chinese Medicine and Pharmacy, Chengdu University of Traditional Chinese Medicine, Chengdu, China

## OPEN ACCESS

### Edited by:

Hai-Jian Sun,  
National University of Singapore,  
Singapore

### Reviewed by:

Katsuya Hirano,  
Kagawa University, Japan  
Omar Estrada,  
Instituto Venezolano de  
Investigaciones Científicas (IVIC),  
Venezuela

### \*Correspondence:

Cheng Peng  
pengchengcxy@126.com  
Hui Ao  
aohui2005@126.com

### Specialty section:

This article was submitted to  
Cardiovascular and Smooth Muscle  
Pharmacology,  
a section of the journal  
Frontiers in Pharmacology

Received: 10 November 2021

Accepted: 24 January 2022

Published: 28 February 2022

### Citation:

Xu J-F, Xia J, Wan Y, Yang Y,  
Wu J-J, Peng C and Ao H (2022)  
Vasorelaxant Activities and its  
Underlying Mechanisms of Magnolia  
Volatile Oil on Rat Thoracic Aorta  
Based on Network Pharmacology.  
*Front. Pharmacol.* 13:812716.  
doi: 10.3389/fphar.2022.812716

**Objective:** Magnolia volatile oil (MVO) is a mixture mainly containing eudesmol and its isomers. This study was to investigate the vasorelaxant effects and the underlying mechanism of MVO in rat thoracic aortas.

**Method:** The present study combined gas chromatography–mass spectrometry (GC-MS) and network pharmacology analysis with *in vitro* experiments to clarify the mechanisms of MVO against vessel contraction. A compound–target network, compound–target–disease network, protein–protein interaction network, compound–target–pathway network, gene ontology, and pathway enrichment for hypertension were applied to identify the potential active compounds, drug targets, and pathways. Additionally, the thoracic aortic rings with or without endothelium were prepared to explore the underlying mechanisms. The roles of the PI3K-Akt-NO pathways, neuroreceptors, K<sup>+</sup> channels, and Ca<sup>2+</sup> channels on the vasorelaxant effects of MVO were evaluated through the rat thoracic aortic rings.

**Results:** A total of 29 compounds were found in MVO, which were identified by GC-MS, of which 21 compounds with a content of more than 0.1% were selected for further analysis. The network pharmacology research predicted that beta-caryophyllene, palmitic acid, and (+)-β-selinene might act as the effective ingredients of MVO for the treatment of hypertension. Several hot targets, mainly involving TNF, CHRM1, ACE, IL10, PTGS2, REN, and F2, and pivotal pathways, such as the neuroactive ligand–receptor interaction, the calcium signaling pathway, and the PI3K-Akt signaling, were responsible for the vasorelaxant effect of MVO. As expected, MVO exerted a vasorelaxant effect on the aortic rings pre-contracted by KCl and phenylephrine in an endothelium-dependent and non-endothelium-dependent manner. Importantly, a pre-incubation with indomethacin (Indo), *N*-nitro-*L*-arginine methyl ester,

**Abbreviations:** 4-AP, 4-aminopyridine; +E, endothelium-intact; -E, Endothelium-denuded; Ach, acetylcholine chloride; CCVDs, cardiac-cerebral vascular diseases; C-T, compound-target; C-T-D, compound-target-disease; C-T-P, compound-target-pathway; Emax, the maximum relaxant magnitude; Et, the real-time relaxant magnitude; GC-MS, gas chromatography-mass spectrometry; Gli, glibenclamide; GO, gene ontology; Indo, Indo-methacin; KATP, ATP-sensitive K<sup>+</sup> channels; KCa<sup>2+</sup>, Calcium-activated K<sup>+</sup> channels; KEGG, Kyoto Encyclopedia of Genes and the Genomes; KIR, Inward rectifier K<sup>+</sup> channels; KV, Voltage-dependent K<sup>+</sup> channels; L-NAME, N-nitro-*L*-arginine methyl ester; MB, methylene blue; MVO, Magnolia volatile oil; PHE, Phenylephrine; PPI, protein-protein interaction; ROCC, receptor-operated Ca<sup>2+</sup> channel; TCM, traditional Chinese medicines; TEA, tetraethyl-ammonium; VDCC, voltage-dependent Ca<sup>2+</sup> channel.

methylene blue, wortmannin, and atropine sulfate as well as 4-aminopyridone diminished MVO-induced vasorelaxation, suggesting that the activation of the PI3K-Akt-NO pathway and  $K_v$  channel were involved in the vasorelaxant effect of MVO, which was consistent with the results of the Kyoto Encyclopedia of Genes and the Genomes. Additionally, MVO could significantly inhibit  $Ca^{2+}$  influx resulting in the contraction of aortic rings, revealing that the inhibition of the calcium signaling pathway exactly participated in the vasorelaxant activity of MVO as predicted by network pharmacology.

**Conclusion:** MVO might be a potent treatment of diseases with vascular dysfunction like hypertension. The underlying mechanisms were related to the PI3K-Akt-NO pathway,  $K_v$  pathway, as well as  $Ca^{2+}$  channel, which were predicted by the network pharmacology and verified by the experiments *in vitro*. This study based on network pharmacology provided experimental support for the clinical application of MVO in the treatment of hypertension and afforded a novel research method to explore the activity and mechanism of traditional Chinese medicine.

**Keywords:** Magnolia volatile oil, network pharmacology, vasorelaxant effect, endothelial dependence and -independence, hypertension

## 1 INTRODUCTION

Hypertension is a pivotal cause for the occurrence of cardiac-cerebral vascular diseases (CCVDs) relevant to complications including stroke, kidney damage, dementia, blindness, myocardial infarction, cancer, and heart failure (August, 2004; Sengul et al., 2016; Volpe et al., 2018; Beaney et al., 2020). It is usually accompanied with pathological characters by the reduction of vasorelaxant capacities and the enhancement of vasoconstrictile reactions responsible for the lack of the blood supply to important organs and tissues (Kizhakekuttu and Widlansky, 2010; Kidoguchi et al., 2021), which is a serious threat to human health, especially for cardiovascular patients. At present, merely 34% of hypertensive patients manage their blood pressure satisfactorily, and their intake of anti-hypertensive medicines is restricted because of their serious adverse reaction to the medicines and the medicines' high cost, especially after they are given continuously to the patients for a prolonged period (Akhtar et al., 2016; Maranta et al., 2017). Thereby, the increasing number of issues prompted the search for alternative and complementary therapies for better treatment of hypertension, which are of higher efficiency, lower cost, and minimal toxicity.

*Magnolia officinalis* Rehd. et Wils. contains phenylpropanoids, lignans, glycosides, alkaloids, flavonoids, essential oil, terpenoids, etc. (Kelm and Nair, 2000), and is a medicinal herb that has been used in the treatment of hyperglycemia (Sun et al., 2015), epilepsy (Chen et al., 2011), dementia (Lee et al., 2012), tumor (Youn et al., 2013), anxiety (Han et al., 2011), and so on. At present, not only the extractions derived from the leaf of *M. officinalis* Rehd. et Wils. but also the main active ingredient ( $\beta$ -eudesmol) in MVO (Obara et al., 2002; Baek, 2004; Lim and Kee, 2005; Yang et al., 2012) are identified to have a vasorelaxant activity. However, little was known about the effect on the potential vascular activity and the mechanisms of oils extracted from the bark of *M. officinalis* Rehd. et Wils. As MVO is a complicated mixture, it is difficult to elucidate its active ingredients and therapeutic mechanisms, which is likely to be related to its

multiple pharmacological activities, biological targets, and pathways. Fortunately, network pharmacology, an innovative and effective approach, is in the light of computational systems pharmacology, which exactly decodes the connections among the herbs, targets, pathways, and diseases at a comprehensive and systematic level (Li, 2016; Yu and Wang, 2016; Luo et al., 2020) and has been successfully applied to study the complex mechanisms of traditional Chinese medicine (TCM) (He et al., 2019). Thereby, the chemical constituents of MVO were analyzed by gas chromatography-mass spectrometry (GC-MS) and the combination of prediction of network pharmacology and verification of rat thoracic aorta was applied to explore the vasorelaxant activity and the underlying mechanisms of MVO. The experiment method was convenient, stable, and reliable, which has been proved by a number of researches (Ferreira et al., 2007; Wang et al., 2015).

In short, to our knowledge, the present study was the first report to holistically reveal the correlation between the mechanisms and the vasorelaxant effect of MVO treatment *via* the combination of network pharmacology prediction and experimental verification, which provided the scientific evidences for the clinical applications of MVO and created a novel direction to explore the activities and mechanisms of TCM.

## 2 MATERIALS

### 2.1 Herbs and Reagents

The bark of *M. officinalis* Rehd. et Wils. was bought from the Chengdu International Trade city of Hehuachi TCM market, which was identified by Chen, an associate professor of the Chengdu University of Traditional Chinese Medicine, as the dry rind of *M. officinalis* Rehd. et Wils. *M. officinalis* Rehd. et Wils. in the experiment was a mixture of equal proportions from seven different habitats, mainly including Chengdu (Sichuan

Province, China), Guiyang (Guizhou Province, China), Anhua (Hunan Province, China), Enshi (Hubei Province, China), Shaoxing (Zhejiang Province, China), Daoxian (Hunan Province, China), and Liu'an (Anhui Province, China).

*N*-hexane and anhydrous sodium sulfate were bought from Sinopharm Chemical Reagent Co., Ltd. Dimethyl sulfoxide was obtained from Chengdu Kelon Chemical Reagent Factory.

## 2.2 Experimental Animals

Male Sprague–Dawley (SD) rats weighing 260–320 g were provided by the Chengdu Dossy Experimental Animals Co., Ltd. (Chengdu, China) [Sichuan Province Animal Use Certificate No. SCXK (Chuan) 2013-15]. All animal care and experimental protocols followed the Animal Management Rules of the Ministry of Health of China. The rats were housed at 25°C, with a 12 h light/dark cycle and with free access to water and food for 5–7 days before the experiments.

## 3 METHODS

### 3.1 The Extraction and Analysis of MVO

#### 3.1.1 Extraction and Preparation of MVO

The bark of *M. officinalis* Rehd. et Wils. was smashed. About 500 g of the sample was added into the original bottom flask (10,000 ml) with 4,000 ml of ultrapure water. MVO samples were prepared by water distillation for 15 h until the oil quantity in the extractor did not increase, obtained from the condenser, and dried over anhydrous sodium sulfate, and finally stored in a sealed and dark glass bottle at 4°C prior to GC-MS analysis.

The calculation formula of MVO extraction rate is as follows:  $ER = V/m \times 100\%$ . ER is the volatile oil extraction rate (%); V is the MVO volume (ml); and m is the weight (g) of the bark of *M. officinalis* Rehd. Et Wils.

#### 3.1.2 GC-MS Analysis of MVO

GC-MS analysis was performed on an Agilent Technologies apparatus 7890A-5975C with HP-INNOWAX MS capillary column (30 m × 250 μm × 0.25 μm). The following oven temperature program was initiated at 60°C, held for 5 min, then increased at the rate of 10°C min<sup>-1</sup>–120°C, held for 0 min, next increased at the rate of 2°C min<sup>-1</sup>–185°C, held for 3 min, and finally increased at the rate of 8°C·min<sup>-1</sup>–250°C. The carrier gas was helium (He) at a constant flow of 1 ml min<sup>-1</sup>. The ion source was kept at 230°C. The splitting ratio was 10:1. The spectrometer operated at 70 eV with the scan from (m/z) 35–550 Da.

### 3.2 Prediction of the Vasorelaxant Activities and The Underlying Mechanisms of MVO Based on Network Pharmacology

#### 3.2.1 Identification of Active Compounds and Prediction of Corresponding Targets of MVO

According to the results of GC-MS, the ingredients with a content of more than 0.1% were screened as the effective ingredients of MVO for in-depth analysis. In the following description, we

called those compounds of MVO “the active compounds of MVO.” The Traditional Chinese Medicine Systems Pharmacology database (TCMSP, <https://tcmsp-e.com/>) was introduced to discover the targets of those compounds. Then, the target names were inputted into the UniProt database (<http://www.uniprot.org/>) with the species selected as “Homo sapiens,” and the gene symbols of the targets were obtained from the UniProt database. In the following description, we called this part of the gene set “the targets of MVO.”

#### 3.2.2 Collection of Targets Related to Hypertension

To ensure the comprehensiveness of hypertension-related genes collected, three databases were selected to search targets. More concretely, the keywords “Hypertension” was inputted in Online Mendelian Inheritance in Man (OMIM, <https://omim.org/>), GeneCards (<http://www.genecards.org/>), and Therapeutic Target Database (TTD, <http://db.idrblab.net/ttd/>) to collect the hypertension-related targets. Afterwards, the obtained targets were also sent to the UniProt database for normalization. Finally, hypertension-related targets were discovered from the above databases after deleting redundancy. In the following description, we called this part of the gene set “genes related to hypertension.”

A Venn diagram was drawn using an online website (<http://bioinformatics.psb.ugent.be/Webtools/Venn/>) to get the same targets between the genes related to hypertension and the target of MVO, which might be the potential targets of MVO in hypertension treatment. In the following description, we called this part of the gene set “overlapping targets of MVO and hypertension.”

#### 3.2.3 Construction of Protein–Protein Interaction Network and Screening of Hub Targets

To figure out the direct and indirect overlapping targets of MVO and hypertension interaction and explore the genes associated with them, the Search Tool for the Retrieval of Interacting Genes (STRING) 11.0 database (<https://string-db.org/>) was employed (Chen et al., 2021). Based on the overlapping targets of MVO and hypertension, we constructed the protein–protein interaction (PPI) network by using the STRING 11.0 database with the species limited to “Homo sapiens” and confidence score >0.4. The topological properties of the PPI network, including the degree, average shortest path length, betweenness centrality, and closeness centrality, were determined in the Cytoscape 3.8.2 (<https://cytoscape.org/>; version 3.8.2). Additionally, the degree value was used to select the putative targets for experimental verification.

#### 3.2.4 Gene Ontology and Pathway Enrichment Analysis

For a better demonstration of the potential biological processes and pathways of MVO in the treatment of hypertension in this study, we utilized the Metascape database (<https://metascape.org/gp/index.html#/main/step1>) to explore the gene ontology (GO) function enrichment analysis, the Kyoto Encyclopedia of Genes and the Genomes (KEGG) pathway enrichment analysis (Yingyao Zhou et al., 2019). The GO terms and pathway

terms with a *P*-value <0.05 were considered as significant enrichment entries.

### 3.2.5 Network Construction and Analysis

In this study, multiple networks were established to visualize and analyze the complicated interconnection of compounds, targets, and diseases in Cytoscape 3.8.2 software. Based on the above results, the compound–target (C–T) network, the compound–target–disease (C–T–D) network, the PPI network, and the compound–target–pathway (C–T–P) network were constructed in Cytoscape 3.8.2 software. In these networks, the nodes of different colors and shapes represented different active compounds, potential targets, or signal pathways, and the edges represented the connections between the nodes.

## 3.3 Verification of the Vasorelaxation Effects and Mechanisms of MVO Through the Isolated Rat Thoracic Aorta Rings

### 3.3.1 Preparation of Solution

Phenylephrine (PHE), acetylcholine chloride (Ach), methylene blue (MB), glibenclamide (Gli), propranolol, atropine sulfate, nifedipine, and N-nitro-L-arginine methyl ester (L-NAME) were prepared with ultrapure water. Indomethacin (Indo) and wortmannin were dissolved in 0.1% DMSO.

The Krebs–Ringer bicarbonate (K-H) solution (118.3 mM NaCl, 4.7 mM KCl, 2.5 mM CaCl<sub>2</sub>, 1.2 mM MgSO<sub>4</sub>, 1.2 mM KH<sub>2</sub>PO<sub>4</sub>, 25 mM NaHCO<sub>3</sub>, 0.5 mM EDTA, and 11.1 mM glucose) (Gao et al., 2007), a calcium-free K-H solution, was prepared by deleting CaCl<sub>2</sub> from the K-H solution and replacing EDTA with EGTA. Notably, CaCl<sub>2</sub> was added at the end after other dissolutions and the solvent was ultrapure water.

### 3.3.2 Preparation of Isolated Thoracic Aorta Rings

Rats were anesthetized with 10% chloral hydrate and isolated the main thoracic aorta immediately, and the arteries were immersed in a cold oxygenated K-H solution. The arteries were cleared of connective tissues and cut into ring segments, 3–4 mm long. The rings were immersed in a temperature-controlled (37°C) chamber bath containing 20 ml K-H solution. During the course of the whole experiment, the solution was continuously oxygenated with a gas mixture of 95% O<sub>2</sub> plus 5% CO<sub>2</sub>. The rings were equilibrated for 1 h at a resting tension of 1 g. During the equilibration period, the K-H solution was changed every 15 min. Then, the rings were contracted with 60 mM KCl and the process was repeated three times to stimulate the maximum contraction.

For de-endothelialized rings, the thoracic arteries were perfused with 0.1% Triton X-100 (0.1% Triton X-100 solution was obtained by dissolving 1 ml Triton X-100 into 100 ml ultrapure water) for 10 s to remove the endothelium before being cutting into ring segments (Fountain et al., 2004; Wang et al., 2015). The integrity of the functional endothelium was tested by obtaining a relaxation to Ach (1 μM) in rings precontracted with PHE (10 μM). The endothelium was considered intact when such an Ach-induced relaxation was more than 85% of the pre-contraction value to PHE. In the

experiments with de-endothelialized rings, the lack of relaxation or no more than 10% in response to Ach was considered to show the successful removal of the endothelium (Wang et al., 2015).

In all aortic ring experimental protocols, the concentrations represent the final tissue chamber concentration (containing 20 ml K-H solution).

### 3.3.3 The Direct Effect of MVO on Resting Endothelium-Intact(+E) Rings

To observe the direct effect of MVO on the isolated rat aorta under normal conditions, an increasing concentration of MVO was added accumulatively (1.5, 2.25, 3, 3.75, and 4.5 μg/ml) to act directly on the +E rings in the MVO group after the initial equilibration of the suspended aortic rings. Similarly, an equal volume of DMSO was added and the highest cumulative concentration of DMSO was 0.015% (v/v) in the control group. Changes in the tension of aortic rings were recorded, and the relaxation rate was calculated.

### 3.3.4 The Direct Effect of MVO on +E Rings or Endothelium-Denuded(-E) Rings

To determine the vasorelaxant effect of MVO, 60 mM KCl and 10 μM PHE was used to precontract stabilized +E or -E rings. After a sustained contraction was obtained, the concentration-dependent responses induced by MVO (1.5, 2.25, 3, 3.75, and 4.5 μg/ml) were examined. The same volume DMSO was applied, and the highest cumulative concentration of DMSO was 0.015% (v/v) in the control group. Changes in the tension of aortic rings were recorded, and the relaxation rate was calculated.

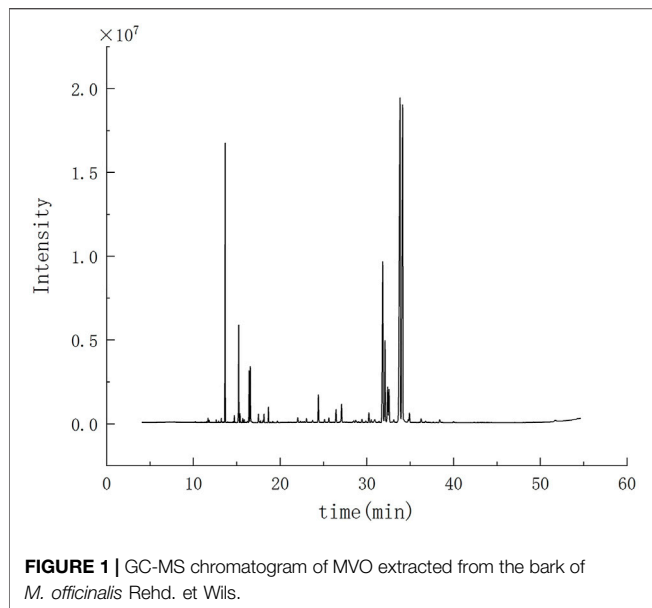
### 3.3.5 Effect of MVO on + E Rings Pre-incubated By With Receptor-Related or Endothelium-Related Inhibitors

To examine the role of a β<sub>2</sub>-adrenoreceptor, muscarinic receptor, and the PI3K-Akt signaling in the vasorelaxant effect of MVO, +E rings were pretreated with 1 μM propranolol (β<sub>2</sub>-adrenoceptor antagonist), 0.1 μM atropine sulfate (a competitive nonselective muscarinic receptor antagonist), and 0.3 μM wortmannin (a PI3K-Akt inhibitor), respectively, for 20 min before the addition of PHE (10 μM). Then, MVO (1.5, 2.25, 3, 3.75, and 4.5 μg/ml) was added. Changes in the tension of aortic rings were recorded, and the relaxation rate was calculated. The vasorelaxant rates were compared with or without inhibitors.

To evaluate the role of the NO-related pathway, known concentrations of the antagonistic agents, involving 100 μM L-NAME (a nonspecific NOS inhibitor), 1 μM Indo (a nonselective cyclooxygenase inhibitor), and 10 μM MB (a cGMP inhibitor) were added to the tissue chamber 20 min before the addition of PHE (10 μM) and KCl(60 mM). Changes in the tension of aortic rings were recorded, and the relaxation rate was calculated. The vasorelaxant rates were compared with or without inhibitors.

### 3.3.6 Effect of MVO on –E Rings Pre-incubated By Various Potassium Channel Blockers

To determine whether MVO-induced relaxation was correlated to the activation of K<sup>+</sup> channels, four kinds of K<sup>+</sup> channel blockers were selected to inhibit the different K<sup>+</sup> channels,



involving  $\text{BaCl}_2$  ( $10^{-3}\text{M}$ ), TEA ( $10^{-3}\text{M}$ ), (Gli  $10^{-6}\text{M}$ ), and 4-AP ( $10^{-3}\text{M}$ ), which were the blockers of  $\text{K}_{\text{IR}}$  (inward rectifier  $\text{K}^+$  channels),  $\text{K}_{\text{Ca}^{2+}}$  (calcium-activated  $\text{K}^+$  channels),  $\text{K}_{\text{ATP}}$  (ATP-sensitive  $\text{K}^+$  channels), and  $\text{K}_{\text{V}}$  (voltage-dependent  $\text{K}^+$  channels), respectively. The -E rings were used in this experiment, pre-incubated with or without those four blockers for 20 min before the addition of PHE ( $10\ \mu\text{M}$ ). The accumulation concentrations of MVO (1.5, 2.25, 3, 3.75, and  $4.5\ \mu\text{g}/\text{ml}$ ) were added after the vasoconstriction of rings became stable. Changes in the tension of aortic rings were recorded, and the relaxation rate was calculated. The vasorelaxant rates were compared with or without blockers.

### 3.3.7 Effect of MVO on Extracellular $\text{Ca}^{2+}$ -induced Contraction and Intracellular $\text{Ca}^{2+}$ Release

To determine whether the vasorelaxation of MVO was resulted from the regulation of  $\text{Ca}^{2+}$  releases,  $\text{KCl}$  ( $60\ \mu\text{M}$ ) and PHE ( $10\ \mu\text{M}$ ) were used to trigger the rings' contraction after pre-incubation with MVO ( $4.5\ \mu\text{g}/\text{ml}$ ), nifedipine ( $4.5\ \mu\text{M}$ ), and DMSO ( $0.015\%$  (v/v)) for 20 min in  $\text{Ca}^{2+}$ -free K-H solution. Changes in the tension of aortic rings were recorded, and the relaxation rate was calculated.

To test the effect of MVO on the regulation of  $\text{Ca}^{2+}$  influx, after pre-contraction with PHE ( $10\ \mu\text{M}$ ) and  $\text{KCl}$  ( $60\ \mu\text{M}$ ) and pre-incubation with MVO ( $4.5\ \mu\text{g}/\text{ml}$ ), nifedipine ( $4.5\ \mu\text{M}$ ), and DMSO ( $0.015\%$  (v/v)) for 20 min, cumulative concentrations of  $\text{CaCl}_2$  ( $0.5$ – $2.5\ \text{mM}$ ) were added in  $\text{Ca}^{2+}$  free K-H solution to trigger the contraction of -E rings. Changes in the tension of aortic rings were recorded, and the relaxation rate was calculated.

### 3.3.8 Data Analysis and Statistics

The formula for calculating the degree of vasodilation was as follows: vasorelaxation rate (VR, %) =  $(\text{Emax} - \text{Et})/\text{Emax} \times 100\%$ . Emax (the maximal relaxant magnitude) was equal to the maximum vasoconstriction force caused by vasoconstrictor. Et (the real-time relaxant magnitude) was equal to the vasoconstriction

force at different concentrations of MVO. Data were presented as mean  $\pm$  S.N. Student's t-test (two-tailed) was used to compare the results in different groups. The difference comparison among multiple groups was tested by one-way ANOVA. A value of  $p < 0.05$  was considered statistically significant.

## 4 RESULTS

### 4.1 The Extraction Rate and Composition Analysis of MVO

There was about 1.55 ml MVO extracted from 500 g of the bark of *M. officinalis* Rehd. et Wils. According to the ER formulation, ER was 0.31%. The results of GC-MS were demonstrated in **Figure 1**. According to total ion chromatography, 29 components were determined, accounting for 95.46% of the total content, which was demonstrated in **Table 1**. Among them, there were 23 compounds with more than 0.1% and the oxygenated sesquiterpenes constituted the main portion of MVO, of which  $\alpha$ -eudesmol,  $\beta$ -eudesmol, and  $\gamma$ -eudesmol were the top three ingredients in MVO with the highest content, accounting for 28.64%, 24.32%, and 10.53%, respectively.

### 4.2 The Results of Network Pharmacology Predictions

#### 4.2.1 Targets of the Active Ingredients of MVO

A total of 23 components of MVO were identified and selected. However, there were 3 ingredients deleted because perillyl aldehyde and (-)-selin-11-en-4 $\alpha$ -ol as well as the target of  $\gamma$ -eudesmol could not be found in the TCMSP database, and 20 other ingredients were selected as the active compounds of MVO for further analysis. Moreover, after the duplicate values were removed, 37 targets of active compounds of MVO were obtained from the TCMSP database and transformed into the gene names *via* the Uniprot database. The detailed information of the active compounds of MVO was listed in **Supplementary Table S1**.

#### 4.2.2 The Construction and Analysis of the C-T Network

The C-T network was built by mapping 20 active compounds to their 37 corresponding potential targets to get a systematic and holistic interaction between the active compounds of MVO and their potential targets. As shown in **Figure 2A**, the network consisted of 58 nodes (1 herbal medicine node, 20 main compound nodes, and 37 compound-associated target nodes) and 190 interaction edges. In the network, the degree of eight compounds was more than 10. In detail, beta-caryophyllene (degree 17), palmitic acid, and (+)- $\beta$ -selinene (degree 14), bicyclo [7.2.0]undec-4-ene,4,11,11-trimethyl-8-methylene-, (1R,4Z,9S)- (degree 13), maryophyllene oxide,  $\alpha$ -muurolene,  $\alpha$ -selinene, and 2-isopropenyl-4a,8-dimethyl-1,2,3,4,4a,5,6,7-octahydronaphthalene (degree 11) presented the maximum interactions with potential targets, revealing that these compounds with high degree values might exert an important role in the potential pharmacological effects of MVO. Moreover, five targets with degrees more than 10 were found, including

**TABLE 1** | The chemical compositions in MVO extracted from the bark of *M. officinalis* Rehd. et Wils.

CAS number	Chemical name	Molecular formula	Remain time/min	The content of MVO/%
17,699-14-8	$\alpha$ -cubebene	C <sub>15</sub> H <sub>24</sub>	11.692	0.1
629-62-9	Pentadecane	C <sub>15</sub> H <sub>32</sub>	11.833	0.05
78-70-6	Linalool	C <sub>10</sub> H <sub>18</sub> O	12.633	0.07
118-65-0	Bicyclo [7.2.0]undec-4-ene,4,11,11-trimethyl-8-methylene-, (1R,4Z,9S)-	C <sub>15</sub> H <sub>24</sub>	13.21	0.14
87-44-5	Caryophyllene	C <sub>15</sub> H <sub>24</sub>	13.674	9.6
488-05-1	Eisholtzia ketone	C <sub>10</sub> H <sub>14</sub> O <sub>2</sub>	14.586	0.05
6753-98-6	$\alpha$ -humulene	C <sub>15</sub> H <sub>24</sub>	15.227	3.45
103,827-22-1	2-isopropenyl-4a,8-dimethyl-1,2,3,4,4a,5,6,7-octahydronaphthalene	C <sub>15</sub> H <sub>24</sub>	15.38	0.28
30,021-74-0	$\gamma$ -muurolene	C <sub>15</sub> H <sub>24</sub>	15.686	0.14
17,066-67-0	(+)- $\beta$ -selinene	C <sub>15</sub> H <sub>24</sub>	16.433	1.86
473-13-2	$\alpha$ -selinene	C <sub>15</sub> H <sub>24</sub>	16.568	2.08
483-76-1	(+)- $\delta$ -cadinene	C <sub>15</sub> H <sub>24</sub>	17.498	0.35
25,532-79-0	Trans- $\alpha$ -bisabolene	C <sub>15</sub> H <sub>24</sub>	17.992	0.09
2111-75-3	Perillyl aldehyde	C <sub>10</sub> H <sub>14</sub> O	18.139	0.35
73,209-42-4	(+/-)-trans-calamanene	C <sub>15</sub> H <sub>22</sub>	19.668	0.09
21,391-99-1	$\alpha$ -calacorene	C <sub>15</sub> H <sub>20</sub>	22.356	0.06
1139-30-6	Caryophyllene oxide	C <sub>15</sub> H <sub>24</sub> O	24.415	1.43
19,888-34-7	(1R,3Z,7Z,11S)-1,5,5,8-tetramethyl-12-oxabicyclo [9.1.0]dodeca-3,7 -diene	C <sub>15</sub> H <sub>24</sub> O	26.45	0.71
913,176-41-7	Caryophyllenyl alcohol	C <sub>15</sub> H <sub>26</sub> O	27.068	1.01
77-53-2	Cedrol	C <sub>15</sub> H <sub>26</sub> O	29.438	0.2
1209-71-8	$\gamma$ -eudesmol	C <sub>15</sub> H <sub>26</sub> O	31.832	10.53
17,334-55-3	(+)-calarene	C <sub>15</sub> H <sub>24</sub>	32.091	4.84
31,983-22-9	$\alpha$ -muurolene	C <sub>15</sub> H <sub>24</sub>	32.379	2.21
23,811-08-7	Hinesol	C <sub>15</sub> H <sub>26</sub> O	32.55	1.96
473-16-5	$\alpha$ -eudesmol	C <sub>15</sub> H <sub>26</sub> O	33.65	28.64
473-15-4	$\beta$ -eudesmol	C <sub>15</sub> H <sub>26</sub> O	34.138	24.32
5945-72-2	(-)-selin-11-en-4 $\alpha$ -ol	C <sub>15</sub> H <sub>26</sub> O	34.908	0.58
19,431-79-9	5 $\alpha$ -hydroxycaryophylla-4(12),8(13)-diene	C <sub>15</sub> H <sub>24</sub> O	36.702	0.14
57-10-3	Palmitic acid	C <sub>16</sub> H <sub>32</sub> O <sub>2</sub>	51.754	0.13

GABRA1 (degree 19), CHRM1 (degree 14), PTGS2 (degree 13), CHRM2 (degree 12), and CHRM3 (degree 11). Each target was connected with a variety of compounds. The C-T network revealed intimate communications between those compounds and their related targets, providing a reference to further investigate the pharmacological mechanisms of MVO.

#### 4.2.3 The Construction and Analysis of the C-T-D Network

A total of 8,983 targets associated with hypertension were identified from the GeneCards, OMIM, and TTD databases after duplicate targets were deleted (Supplementary Table S1). And then, the Venn graph was built, as pictured in Figure 2B. Furthermore, according to the 30 overlapping targets of MVO and hypertension, the C-T-D network was constructed, which consisted of 54 nodes (1 hypertension node and one herbal medicine note and 52 overlapping target nodes) and 214 edges. As shown in Figure 2C, the top nine targets with the degree values  $\geq 10$  were regarded as the most pivotal targets in the C-T-D network, namely, GABRA1, CHRM1, PTGS2, CHRM2, CHRM3, SLC6A2, GABRA6, NCOA2, and GABRA2. Thereby, the above targets might be the potential targets for MVO to treat hypertension.

#### 4.2.4 The Construction and Analysis of PPI Network

The PPI network was constructed to better interpret the mechanisms of MVO in hypertension treatment by using STRING software, as shown in Figure 2B. Thirty overlapping targets were used to establish

a PPI network after importing into the STRING database. As shown in Figure 2D, the PPI network consisted of 27 nodes and 70 edges. Based on the degree principle of each target, TNF, CHRM1, ACE, IL10, PTGS2, REN, F2, SLC6A3, GABRA6, GRIA2, CHRNA7, GABRA1, CHRM2, and GABRA2 were determined as the hub's top 14 targets. Moreover, we assessed the associations between hub targets and hypertension by the Genecards database. As it was shown in Figure 2E, these hub targets were closely corresponded with hypertension according to gifts.

#### 4.2.5 The Analysis of Gene Ontology Enrichment and Construction of C-T-P Network

To explore the functional role of the 30 overlapping targets, GO functional analysis were conducted via the Metascape database. The results of GO enrichment analysis involved 48 cell components (CCs), 50 molecular functions (MFs), and 286 biological processes (BPs) with a threshold value of  $p < 0.05$ . The top GO analysis results are shown in Figures 2F-H. The CC analysis demonstrated that the overlapping targets were mainly related to the postsynaptic membrane, membrane raft, side of the membrane, apical part of a cell, plasma membrane signaling receptor complex, endoplasmic reticulum lumen, and endocytic vesicle. The MF results mainly included postsynaptic neurotransmitter receptor activity, acetylcholine receptor activity, protease binding, cation transmembrane transporter activity, endopeptidase activity, symporter activity, protein homodimerization activity, and protein domain specific binding. The BP results mainly comprised of

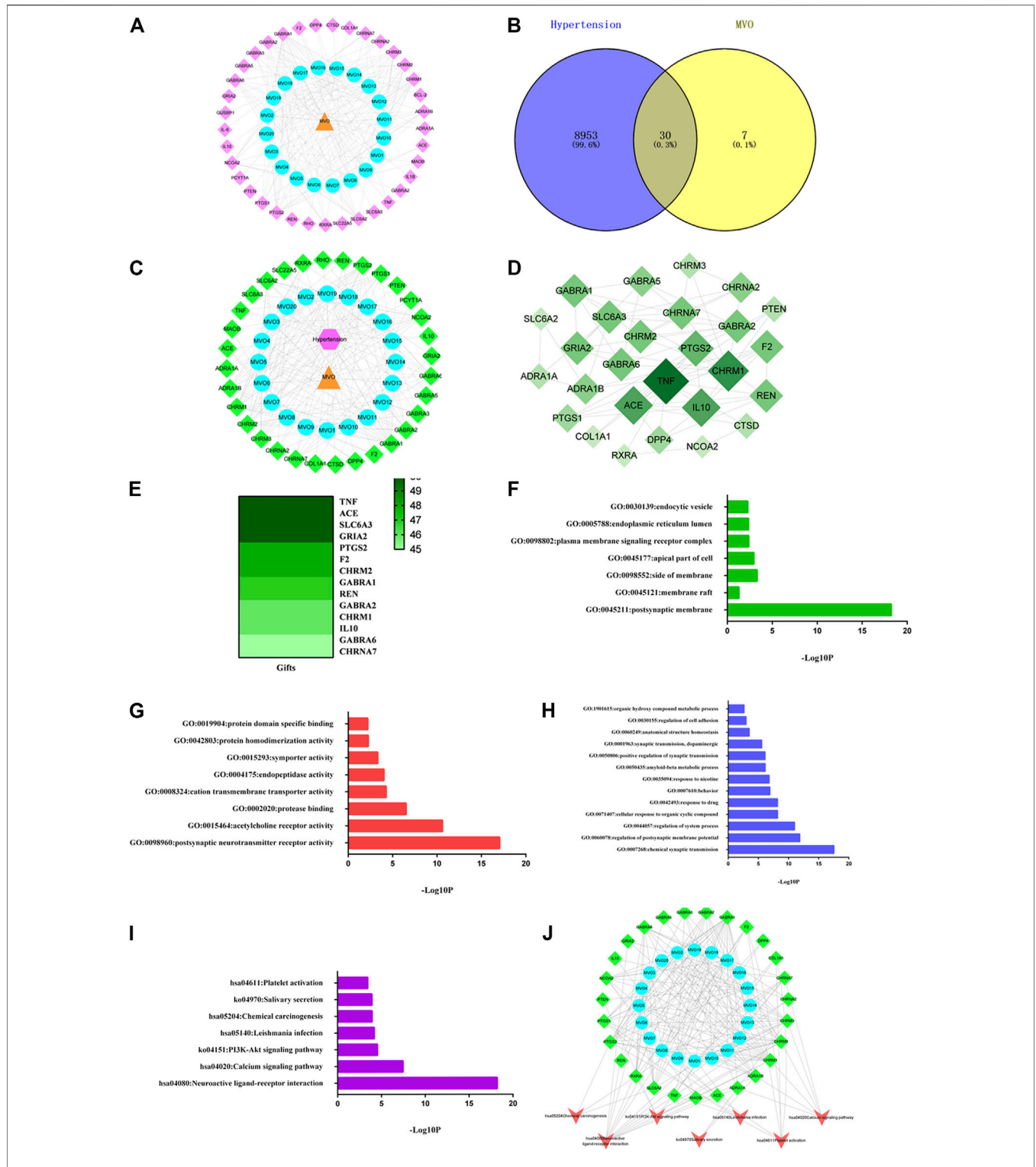
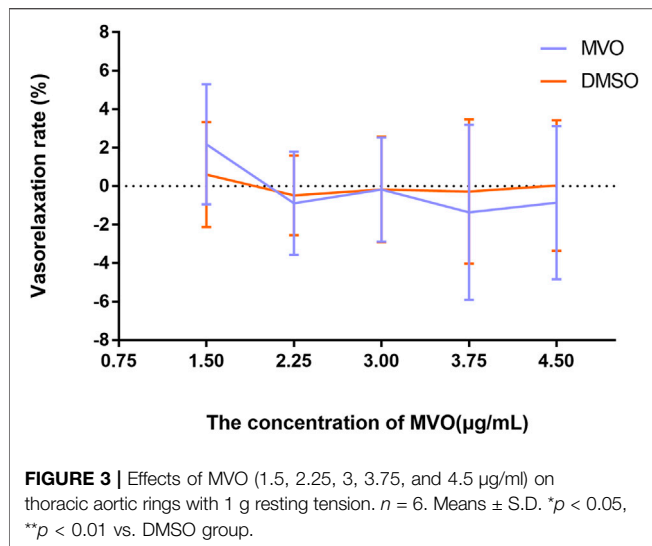


**FIGURE 2 |** MVO potential target-hypertension target network and analysis. **(A)** The C-T network of MVO. **(B)** The Venn diagram. **(C)** The C-T-D network of MVO. **(D)** The PPI network of the 30 overlapping targets. **(E)** The heatmap of gifts between hypertension and hub target. **(F)** The GO-CC enrichment analysis. **(G)** The GO-MF enrichment analysis. **(H)** The GO-BP enrichment analysis. **(I)** The KEGG enrichment analysis. **(J)** The C-T-P network of MVO. The orange triangle node represented MVO, the blue circle node represented each compound of MVO, the pink diamond node represented the targets of MVO, the pink hexagon refers to hypertension, and the green diamond node represented the overlapping targets of MVO and hypertension; the red V was the symbol of pathways.



chemical synaptic transmission, the regulation of postsynaptic membrane potential, regulation of system process, cellular response to organic cyclic compound, response to drug, behavior, response to nicotine, amyloid-beta metabolic process, positive regulation of synaptic transmission, synaptic transmission, dopaminergic, anatomical structure homeostasis, regulation of cell adhesion, and organic hydroxy compound metabolic process.

The results of the KEGG enrichment analysis revealed that seven pathways met the threshold value of  $p < 0.05$  after sorting according to the  $P$ -value. As depicted in **Figure 2I**, the KEGG pathways of MVO against hypertension were mainly related to neuroactive ligand–receptor interaction, the calcium signaling pathway, PI3K–Akt signaling pathway, Leishmania infection, chemical carcinogenesis, salivary secretion, and platelet activation.

The results of the C-T-P network were demonstrated in **Figure 2J**. There were 54 nodes and 199 edges in the C-T-P network, including 20 active compounds of MVO nodes, 27 overlapping target notes, and seven pathway nodes. The top three degrees were neuroactive ligand–receptor interaction (degree = 13), the calcium signaling pathway and platelet activation (degree = 6), and PI3K–Akt signaling pathway (degree = 5), respectively, which might be mainly responsible for the vasorelaxant effect of MVO.

## 4.3 The Results of Vasorelaxation Effects and Mechanisms of MVO

### 4.3.1 Effects of MVO on Thoracic Aortic Rings With 1 g Resting Tension

The accumulative addition of MVO (1.5, 2.25, 3, 3.75, and 4.5 µg/ml) had no significant effects on rat thoracic aortic rings-sustained basal tension when compared to the vehicle control group ( $p > 0.05$ ) (**Figure 3**).

### 4.3.2 Effects of MVO on +E Rings Pre-contracted By KCl and PHE

In **Figure 4**, MVO produced relaxation in +E rings in a concentration-dependent manner pre-contracted with PHE

(**Figure 4A**) and KCl (**Figure 4B**). When the rings contracted with PHE (10 µM), the  $E_{max}$  for MVO was  $54.97\% \pm 3.03\%$ , and the PHE-DMSO was  $15.15\% \pm 3.66\%$  (**Figure 4C**). Additionally, when the rings contracted with KCl (60 mM), the  $E_{max}$  for MVO was  $91.96\% \pm 5.38\%$ , while the  $E_{max}$  for DMSO was  $9.93\% \pm 5.92\%$  (**Figure 4D**). In conclusion, the statistical differences were shown in arterial rings with the control group compared with the treatment of KCl/PHE-MVO groups (\*\* $p < 0.01$ ), revealing that MVO elicited concentration-dependent relaxations in the arterial segments precontracted by KCl or PHE under +E conditions.

### 4.3.3 Vasorelaxant Effect of MVO on -E and +E Rings Pre-contracted By KCl and PHE

Compared with VR in rings with endothelium, the vasorelaxant effects of MVO obviously decreased and were statistically significant in -E arterial rings (**Figure 5**). The VR of -E-KCl-MVO decreased by about 25% ( $E_{max}/KCl$ : +E,  $91.96\% \pm 5.38\%$  vs. -E,  $65.74\% \pm 3.27\%$ ,  $p < 0.01$ ), and the VR of -E-PHE-MVO decreased by about 5% ( $E_{max}/PHE$ : +E,  $54.97\% \pm 3.03\%$  vs. -E,  $49.58\% \pm 3.31\%$ ,  $p < 0.05$ ).

### 4.3.4 Vasorelaxant Effect of MVO on +E Rings Pre-incubated By Receptor-Related Inhibitors

Pre-incubation with propranolol (1 µM) did not significantly regulate MVO-produced vasorelaxation ( $E_{max}$ :  $50.65\% \pm 4.43\%$  vs.  $54.97\% \pm 3.03\%$  in the PHE-MVO group,  $p > 0.05$ , which was depicted in **Figure 6A**, suggesting minimal contribution by  $\beta$ -adrenoceptors to the MVO-induced vasorelaxation.

Pre-incubation with atropine sulfate (1 µM), a muscarinic receptor antagonist, did downregulate MVO-produced vasorelaxation ( $E_{max}$ :  $32.87\% \pm 4.33\%$  vs.  $54.97\% \pm 3.03\%$ ,  $p < 0.01$ ) (**Figure 6B**), which proved that the M receptor was responsible for the vasorelaxant effect of MVO.

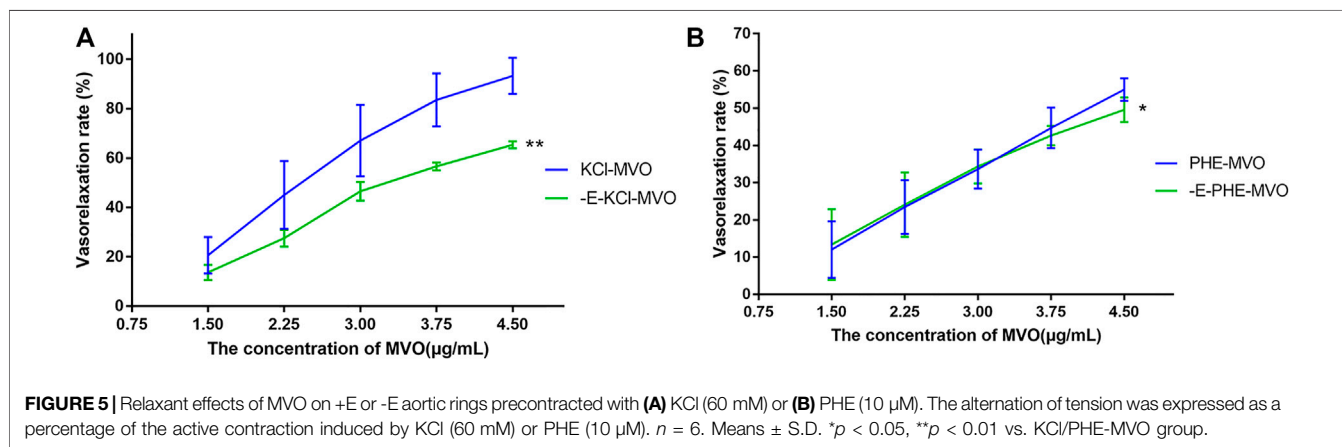
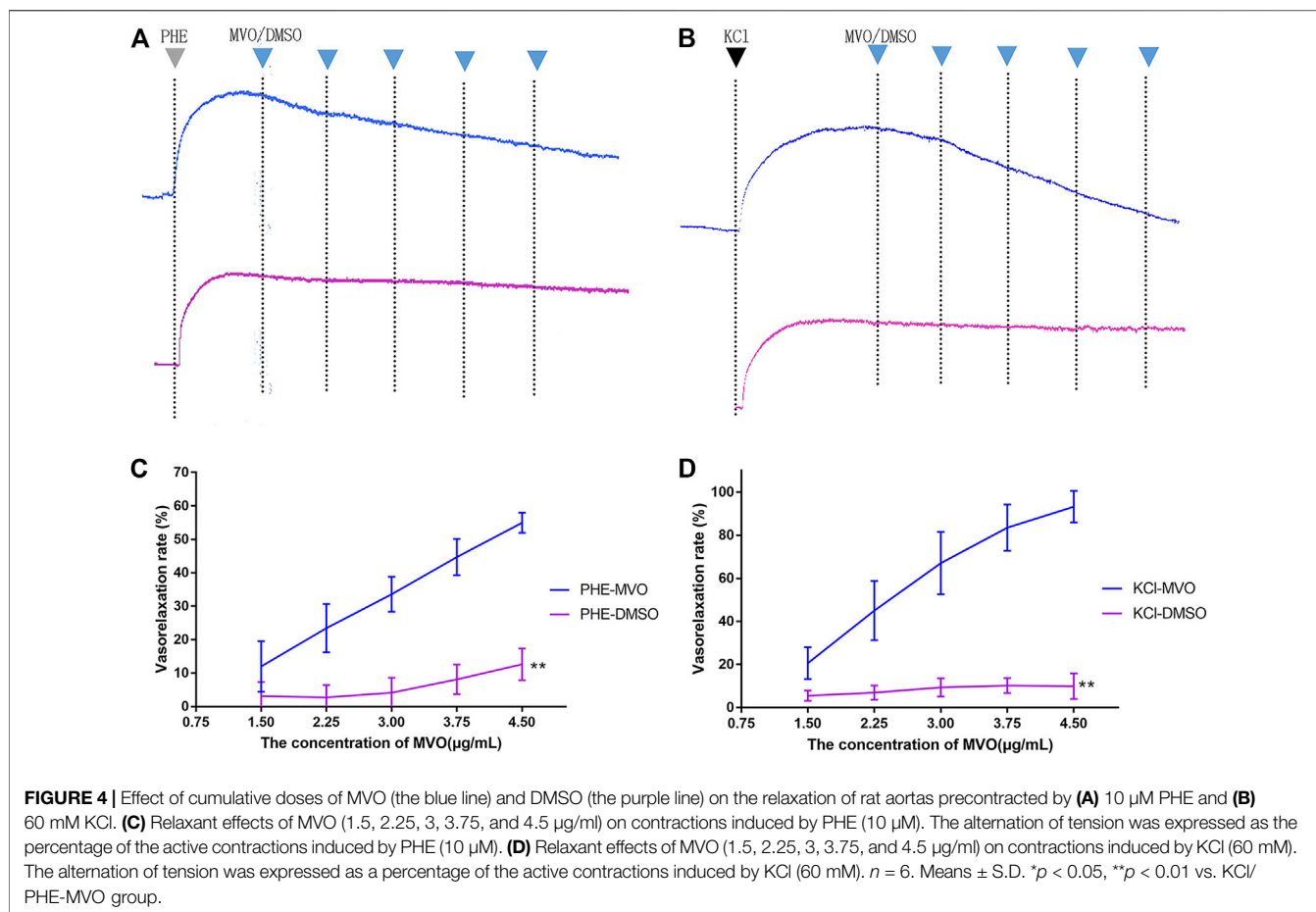
### 4.3.5 Vasorelaxant Effect of MVO on +E Rings Pre-incubated By Endothelium-Related Inhibitors

Pre-incubation with wortmannin (0.3 µM) did significantly downregulate MVO-produced vasorelaxation ( $E_{max}$ :  $54.97\% \pm 3.03\%$  vs.  $32.8\% \pm 3.57\%$ ,  $p < 0.01$ ) (**Figure 7A**), which demonstrated that PI3K–Akt might play a vital role in the MVO vasorelaxant effect.

As displayed in **Figure 7B**, the pre-incubation of +E arterial rings with Indo, L-NAME, or MB did inhibit MVO-produced relaxation ( $E_{max}/KCl$ -Indo: +E,  $70.35\% \pm 7.59\%$ ,  $p < 0.05$ ;  $E_{max}/KCl$ -MB: +E,  $57.26\% \pm 4.61\%$ ,  $p < 0.05$ ;  $E_{max}/KCl$ -L-NAME: +E,  $79.48\% \pm 6.35\%$ ,  $p < 0.05$ ) vs. the KCl-MVO group. Similarly, pre-contraction with PHE and pre-incubation with L-NAME or MB did inhibit MVO-produced relaxation ( $E_{max}/PHE$ -L-NAME: +E,  $36.51 \pm 3.49\%$ ;  $E_{max}/PHE$ -MB: +E,  $38.72 \pm 1.03\%$ ;  $p < 0.01$ ). On the contrary, Indo did accelerate MVO-induced relaxation precontracted by PHE ( $E_{max}/PHE$ -Indo: +E,  $64.37 \pm 5.23\%$ ,  $p < 0.01$ ) vs. the PHE-MVO group shown in **Figure 7C**.

### 4.3.6 Vasorelaxant Effect of MVO on -E Rings Pre-incubated By Various Potassium Channel Blockers

After pre-incubation with TEA (10 mM), Gli (10 µM), or BaCl<sub>2</sub> (100 µM) for 20 min, the  $E_{max}$  values that MVO produced were

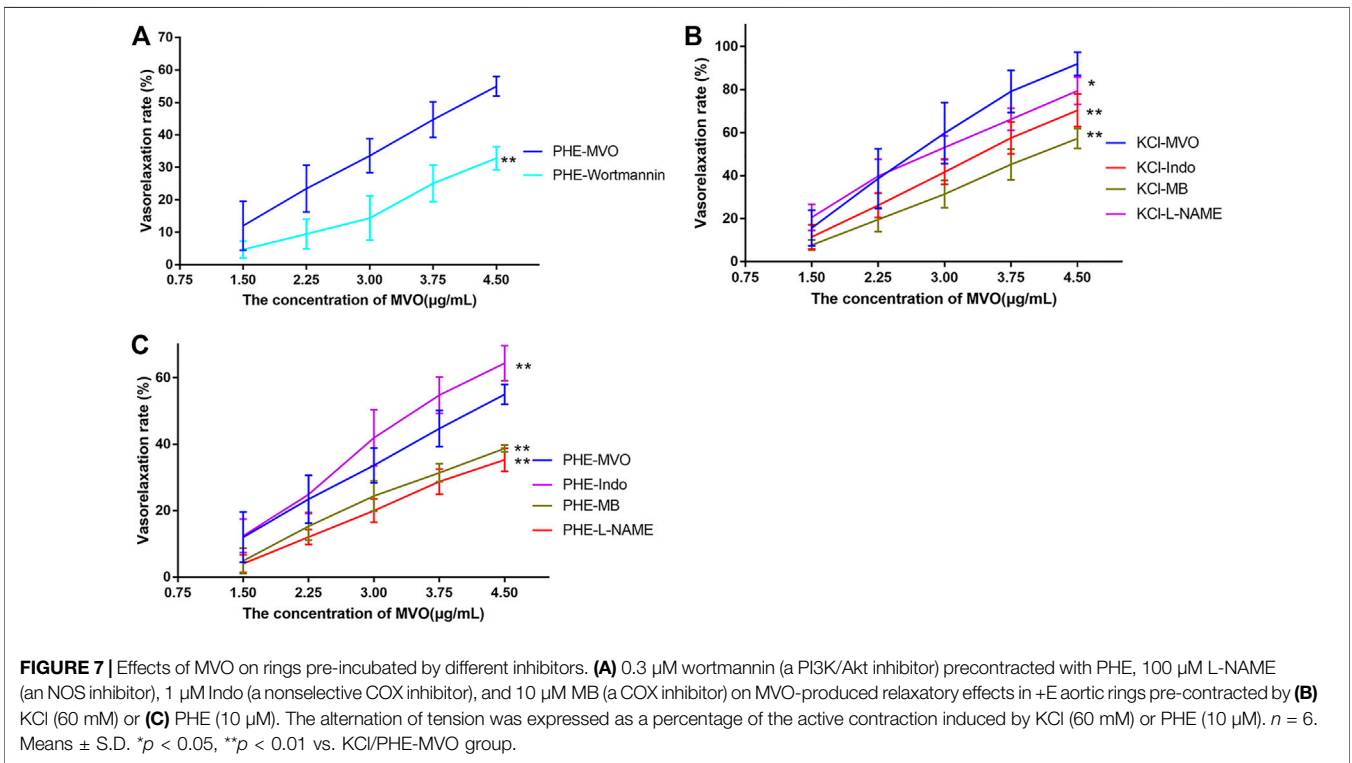
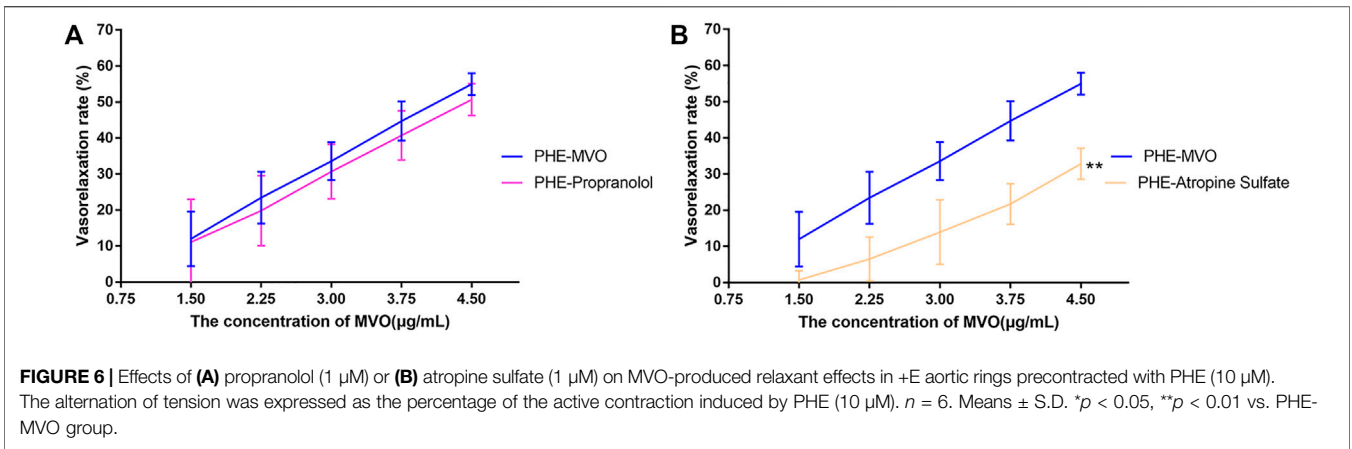


44.71%  $\pm$  0.99%, 53.45%  $\pm$  6.26%, and 52.69%  $\pm$  4.01%, respectively, which had no statistical significance as compared to the -E-PHE-MVO group ( $E_{max}$  49.58  $\pm$  3.31%,  $p > 0.05$ ), suggesting that  $K_{Ca}$ ,  $K_{ATP}$ , and  $K_{IR}$  did not participate in the vasorelaxant effect of MVO. In contrast, after the pre-incubation of 4-AP (1 mM) for 20 min, the  $E_{max}$  values that MVO produced were 37.31  $\pm$  6.16%, which had a statistical significance as compared to the -E-PHE-MVO group ( $E_{max}$  49.58  $\pm$  3.31%,

$p < 0.05$ ) (Figure 8), showing that the activation of Kv channel participated in the vasorelaxant effect of MVO in this study.

### 4.3.7 Effect of MVO on -E Rings in $Ca^{2+}$ -free K-H Solution

In a  $Ca^{2+}$ -free solution, there was no significant difference between MVO and the DMSO group in the short-term contraction caused by PHE (Figures 9A,C) or KCl (Figures



9B,E) (*p* > 0.05). Compared with the Ca-Nifedipine-PHE group, there was a significant difference in the Ca-MVO-PHE group (*p* < 0.01). The above results suggested that MVO relaxed aortic rings without releasing calcium from the sarcoplasmic reticulum.

In a Ca<sup>2+</sup>-free solution, the accumulative addition of CaCl<sub>2</sub> induced concentration-dependent contractions of -E aortic rings depolarized with 10 μM PHE or 60 mM KCl. Pretreatment with 4.5 μg/ml MVO and nifedipine could significantly antagonize Ca<sup>2+</sup>-induced contractions, which was shown in Figures 9A,B. Among them, there was a statistical difference between the CaCl<sub>2</sub>-MVO-PHE group (29.63 ± 5.45%) and the CaCl<sub>2</sub>-DMSO-PHE group (40.98 ± 1.47%), *p* < 0.01 (Figure 9D). In addition, the CaCl<sub>2</sub>-MVO-

KCl group (11.82 ± 3.92%) showed a significant difference from the CaCl<sub>2</sub>-DMSO-KCl group (23.95 ± 4.34%) and the CaCl<sub>2</sub>-nifedipine-KCl group (-3.14 ± 4.16%), (*p* < 0.01) (Figure 9F). Therefore, these results showed that MVO exerted a vasorelaxant effect by inhibiting external calcium influx to a certain extent.

## 5 DISCUSSION

The present study explored the vasorelaxant activity of MVO in rat aorta. The compounds of MVO were initially analyzed by GC-MS technology, and network pharmacology analysis was applied

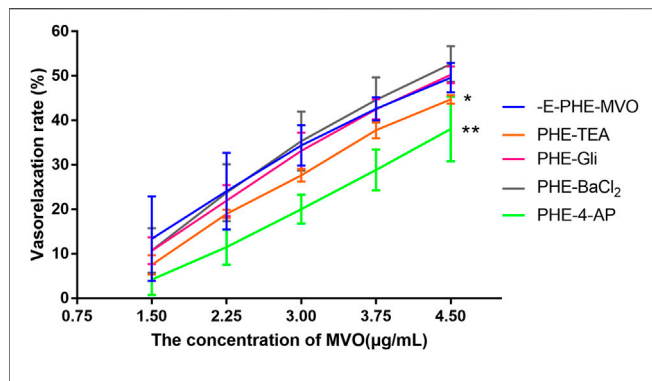


**FIGURE 8** | Influences of different  $K^+$  channel inhibitors, including  $Ca^{2+}$ -activated  $K^+$  ( $K_{Ca}$ ) channel inhibitor TEA (10 mM), voltage-dependent  $K^+$  ( $K_V$ ) channel inhibitor 4-AP (1 mM), ATP-sensitive  $K^+$  ( $K_{ATP}$ ) channel inhibitor glyburide (10  $\mu$ M), and inward rectifier  $K^+$  ( $K_{IR}$ ) channel inhibitor  $BaCl_2$  (100  $\mu$ M) on MVO-produced relaxant effects in -E aortic rings precontracted with PHE (10  $\mu$ M). The alternation of tension was expressed as the percentage of the active contraction induced by PHE (1  $\mu$ M).  $n = 6$ . Means  $\pm$  S.D. \* $p < 0.05$ , \*\* $p < 0.01$  vs. -E-PHE-MVO group.

to predict the active ingredients, the targets, the biological processes, and the pathways of MVO on hypertension. The perfusion experiment of the isolated thoracic aortic ring was selected to verify the predictions of network pharmacology.

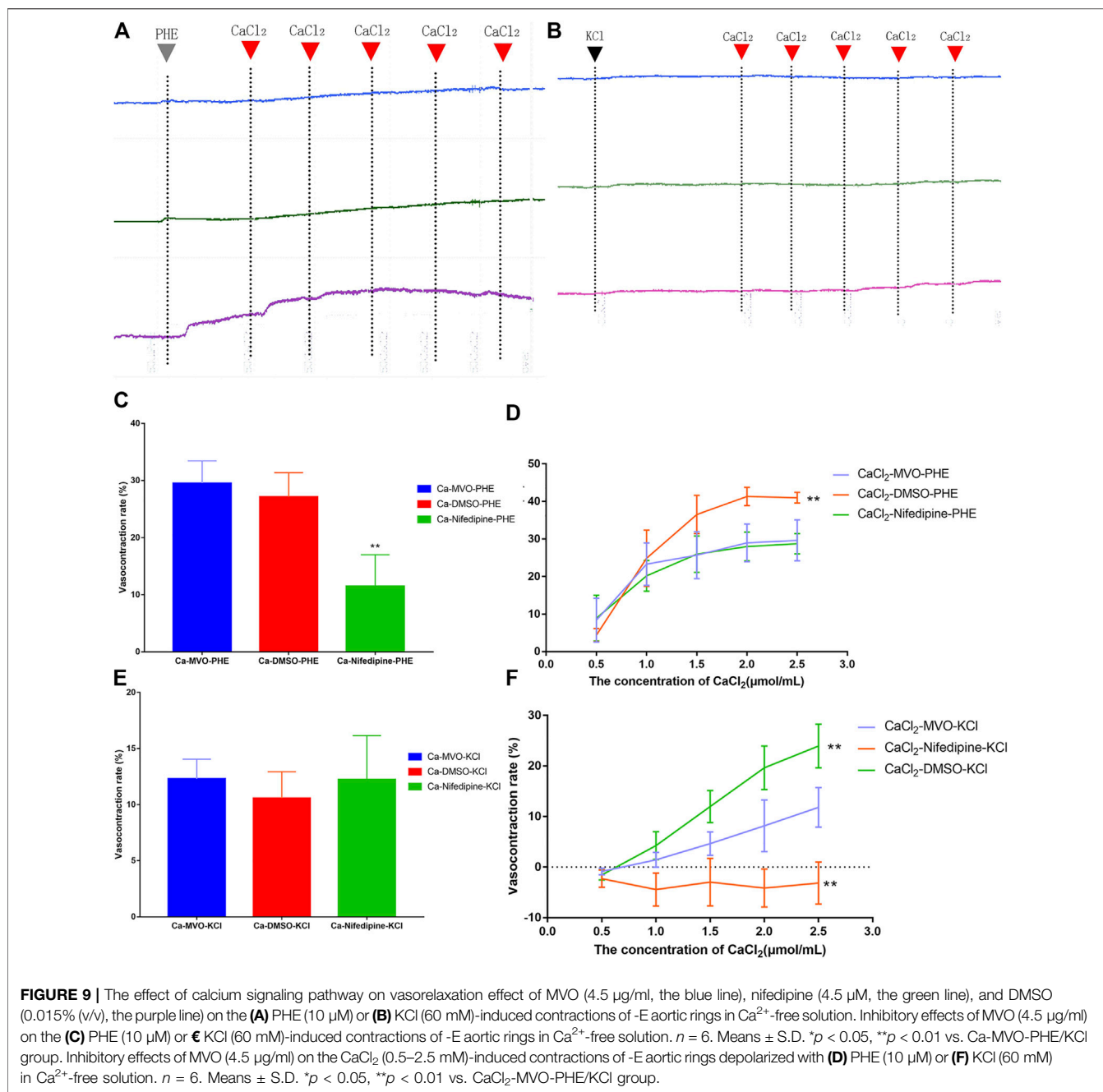
There may be quality differences between Chinese herbs from different habitats. Thus, to avoid the influence of the quality of the tested medicinal materials on the experimental results, the dry rind of *M. officinalis* Rehd. et Wils. from seven different main producing areas were mixed in equal proportions as experimental medicinal materials. According to GC-MS results, the composition of MVO was consistent with that in other studies. For example, our study demonstrated that  $\alpha$ -,  $\beta$ -, and  $\gamma$ -eudesmol were the main ingredients of MVO, and the ingredients with considerably higher contents were mainly  $\beta$ -caryophyllene, (+)-calarene, and  $\alpha$ -humulene (Yang et al., 2007; Xu et al., 2009; Lou et al., 2011; Fang et al., 2012; He et al., 2012; Tang et al., 2019), suggesting that the quality of MVO in our study was representative and reliable. Previous studies have found that  $\beta$ -caryophyllene is a type of bicyclic sesquiterpenoids that has good application value in cardiovascular and cerebrovascular diseases by eliciting anti-inflammatory (Basha and Sankaranarayanan, 2016) and neuroprotective effects (Zhang et al., 2017; Machado et al., 2018), which are directly and indirectly related to vascular disease and hypertension (Ohbuchi et al., 2015; Scholl et al., 2015; Jiye Chen et al., 2021). Then, those ingredients in MVO were used to explore its vasorelaxant activity and mechanisms *via* network pharmacology. For one thing, although  $\alpha$ -,  $\beta$ -, and  $\gamma$ -eudesmol had the highest content of MVO, they were not the active ingredients predicted by network pharmacology. For another thing, although  $\alpha$ -caryophyllene was regarded as one of the most possible ingredients to vasorelaxant vessels proved by network pharmacology, its vasorelaxant effect has not been confirmed. Moreover, the results showed that the same target was connected to multiple ingredients in MVO, suggesting that the active ingredients in MVO were likely to have an interaction

with the treatment of hypertension. Therefore, MVO, rather than beta-caryophyllene or other monomer compounds, was used to do experiments *in vitro*.

In the PPI network, a total of 14 targets, such as TNF, CHRM1, ACE, IL10, PTGS2, REN, and F2, were the hub targets of MVO for treating hypertension. Studies have shown that those targets are closely related to thrombus formation and inflammation, which are involved in the development of hypertension (Otterdal et al., 2008). Long-term inflammation can increase the production of ROS, cause oxidative stress and endothelial dysfunction, (Zhang et al., 2018) and easily result in hypertension (Fujita, 2014; Gomolak and Didion, 2014). Furthermore, the inflammation is characterized by increased levels of local inflammatory cytokines such as TNF (Davis et al., 2002), IL10 (Di et al., 2020), and PTGS2 (Simon, 1999), which are more likely to be useful diagnostic tools for hypertension in the future. Above all, these results provide preliminary evidence for illuminating the multi-targeted mechanisms of the anti-hypertensive effect of MVO.

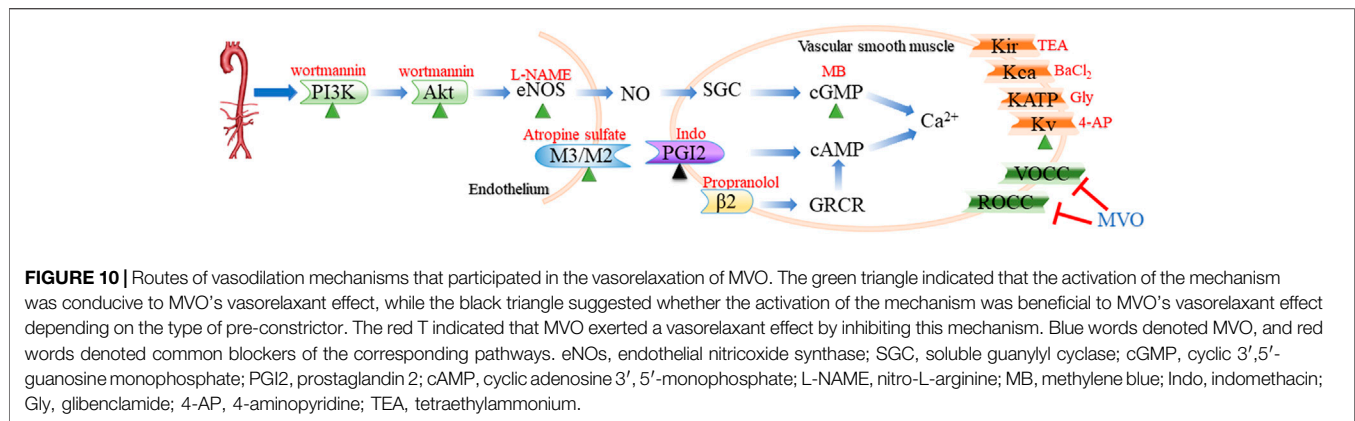
In the KEGG pathway analysis, overlapping targets' enrichment in hypertension-associated pathways mainly included neuroactive ligand-receptor interaction, the PI3K-Akt signaling pathway, and calcium signaling pathway, which played a vital role in the management of hypertension. Substantial evidence has shown that the treatment of hypertension was closely regulated by the activation of the Src-PI3K/Akt-eNOS signaling pathway (Hao et al., 2017) and blockage of the  $Ca^{2+}$  channel (Zhou et al., 2019), which were consistent with the prediction of network pharmacology. Although network pharmacology analysis is a widely used and acceptable method to predict the therapeutic mechanism, it is necessary to confirm the correctness of the prediction due to the possible different standards and spurious associations between one database and another (Luo et al., 2020). The first step was to verify whether MVO had a vasodilator function and whether this function was related to the function of these predicted targets and pathways. Thus, it is vital for us to carry out *in vitro* vasodilatory experiments.

However, the drawback of the investigation for the mechanism underlying the MVO-induced vasorelaxation was its heavy dependence on the pharmacological inhibitors. Therefore, it was important to make some prediction *via* network pharmacology before the mechanism research. Fortunately, the previous network pharmacology in our study provided directions and clues for the mechanism research, making it more targeted. However, it was worth noting that DMSO has vasodilatory activity at high concentrations (0.1%–3%) (Kaneda et al., 2016). Therefore, as a solvent and control group, it is important to control the concentration of DMSO. Wang et al. (2015) wrote that "The time-matched vehicle control (DMSO) group was also analysed. The final concentration of DMSO was 0.1% (v/v)" in their study. However, DMSO (0.015% v/v) was the highest cumulative concentration of the control group in our study, suggesting that the vasorelaxant activity of the tested solution in the experiment was mainly due to the vasorelaxant effect of MVO instead of DMSO. We firstly evaluated the vasorelaxant effect of MVO in rat thoracic aorta (Zhong Yan



Zhou et al., 2019). As was illustrated in **Figure 4**, MVO relaxed KCl- and PHE-induced vasoconstriction and the vasorelaxation effect was more effective in KCl-contracted rat aorta, which preliminarily showed that MVO exactly exerted a vasorelaxant effect. Secondly, in order to verify the pathways of KEGG, atropine sulfate, a nonselective muscarinic receptor antagonist, was used to verify neuroactive ligand–receptor interaction. Neuronal excitability is directly linked to the ion channel state of the central nervous system, which is closely related to neuronal signaling and the regulation of blood pressure (Scholl et al., 2015). The results showed that there was a significant difference in the VR (%) between the two groups with or without atropine sulfate,

which was shown in **Figure 6B**, revealing that MVO exactly exerted vasorelaxant effects through the activating muscarinic receptors. However, the specific receptor subtype was not clear because atropine sulfate is a competitive nonselective muscarinic receptor antagonist, and the muscarinic limb of the parasympathetic system not only contracts smooth muscle directly *via* activation of M3 receptors (Murthy and Makhlof, 1997) but also abrogates sympathetically mediated relaxation *via* the activation of M2 receptors (Kume and Kotlikoff, 1991). Thirdly, wortmannin and several endothelium-related inhibitors (involving Indo, MB, and L-NAME) were selected to study the effect of the PI3K-Akt-NO pathway. The



motivation of the PI3K-Akt pathway is associated with the phosphorylation of eNOS that causes the production and release of NO, vascular integrity, as well as regulation of blood pressure homeostasis (Peixoto et al., 2017; Lee et al., 2018). Our experiment showed the VR (%) was significantly different in the presence or absence of wortmannin, an inhibitor of the PI3K-Akt signaling involved in the vasorelaxant effect (Hao et al., 2017), suggesting that the activation of the PI3K-Akt pathway was of the MVO to relax aortic rings. Additionally, L-NAME (a nonspecific NOS inhibitor) and MB (a cGMP inhibitor) partly inhibited the vasorelaxation of MVO precontracted by KCl or PHE, which indicated that MVO exerted a vasorelaxant effect through promoting NO release and cGMP activity in part. Notably, Indo (a nonselective cyclooxygenase inhibitor) showed a completely different effect precontracted with PHE and KCl. Compared with the control group, the VR (%) in Indo-PHE was higher than that of the PHE-MVO group, while Indo-KCl was lower than that of KCl-MVO, which might be correlated with their different vasorelaxant mechanisms. In detail, KCl contracted rat rings through depolarizing the membrane, and the opening of the voltage-dependent  $\text{Ca}^{2+}$  channels (VDCCs) (Eichhorn and Dobrev, 2007) while PHE acted on  $\alpha_1$ -adrenoceptors and subsequently motivated receptor-operated  $\text{Ca}^{2+}$  channels (ROCCs) (Lee et al., 2010). In conclusion, the PI3K-Akt-NO pathway might be responsible for the vasorelaxant effect of MVO, which was consistent with the results of KEGG. Lastly, a  $\text{Ca}^{2+}$ -free solution was applied to study whether the activation of calcium ion channels was involved in the vasorelaxant effect of MVO. The constriction of vascular smooth muscle is initiated by an increase of the concentration of  $\text{Ca}^{2+}$  ( $[\text{Ca}^{2+}]_i$ ), and the calcium signaling pathway is expressed in virtually all vascular smooth muscle cells (VSMCs), and they are primarily activated by an elevation of  $[\text{Ca}^{2+}]_i$  due to the change of membrane potential (Pérez et al., 2001; Quilley and Qiu, 2005) or agonist-stimulated (Ganitkevich and Isenberg, 1990)  $\text{Ca}^{2+}$  release from intracellular stores. Importantly, calcium ion channels are divided into VDCCs and ROCCs, which can be activated by KCl and PHE, respectively (Anfinogenova et al., 2004; Thorneloe and Nelson, 2005; Lee et al., 2010). To determine whether the vasorelaxant activity of MVO resulted from the regulation of  $\text{Ca}^{2+}$ , the effect of

MVO on the contractile response induced by PHE and KCl and the addition of  $\text{CaCl}_2$  in  $\text{Ca}^{2+}$ -free solution was studied. As shown in the results, compared with the control group, incubation with MVO caused an almost negligible effect shift of VR (%) in  $\text{Ca}^{2+}$ -free solution precontracted by PHE and KCl, suggesting that the release of  $\text{Ca}^{2+}$  from the sarcoplasmic reticulum played a negligible role in the vasorelaxant activity of MVO. Differently, MVO exerted its vasorelaxant effect *via* inhibiting the external  $\text{Ca}^{2+}$  influx.

Moreover, the removal of endothelium partially attenuated MVO-induced relaxation, suggesting that VSMC-mediated vasodilation mechanisms, including the  $\beta_2$ -adrenoceptor, potassium ion channels, and calcium ion channels (Tang et al., 2021), were likely involved in the vasorelaxant activity of MVO. Therefore, in addition to calcium ion channels, which were predicted by the results of network pharmacology, the effect of  $\beta_2$ -adrenoceptor and potassium ion channels was explored *via* the application of different blockers. For one thing,  $\beta$ -adrenoceptor agonists elicited vasodilatory activity *via* activating adenylyl cyclase and consequently increasing cAMP in VSMCs (Huang and Kwok, 1998). As shown in **Figure 6A**, the  $\beta_2$ -adrenoceptor played no role in the vasorelaxant effect of MVO, which was confirmed by the usage of propranolol. For another thing, there are four kinds of the  $\text{K}^+$  pathway, involving  $\text{K}_{\text{IR}}$  (inward rectifier  $\text{K}^+$  channels),  $\text{K}_{\text{Ca}}$  (calcium-activated  $\text{K}^+$  channels),  $\text{K}_{\text{ATP}}$  (ATP-sensitive  $\text{K}^+$  channels), and  $\text{K}_{\text{V}}$  (voltage-dependent  $\text{K}^+$  channels), which can be blocked by  $\text{BaCl}_2$ , TEA, Gli, and 4-AP, respectively. Among them,  $\text{K}_{\text{V}}$  exerts a dominant effect on determining the resting membrane potential and basal regulation on certain VSMCs (Park et al., 2010). In this study, the vasorelaxant effect of MVO was significantly inhibited by 4-AP, a  $\text{K}_{\text{V}}$  channel blocker. However,  $\text{K}_{\text{ATP}}$ ,  $\text{K}_{\text{Ca}}$ , and  $\text{K}_{\text{IR}}$  played no role in the vasorelaxant effect of MVO, which was confirmed by the usage of Gli, TEA, and  $\text{BaCl}_2$ , respectively.

Collectively, our integrative approach elucidated the potential mechanisms of MVO against hypertension based on a systematic network perspective, and the novel findings regarding an acute vasorelaxant effect of MVO were demonstrated (**Figure 10**). According to the results of network pharmacology and experiment *in vitro*, MVO induced the relaxation of arterial rings in a dose-dependent manner endothelium dependently

and independently, which were identified by the following four observations: 1) PI3K-Akt-NO-related and muscarinic receptor-related mechanisms were responsible for MVO-induced vasorelaxation partially; 2) the  $K_V$  channel participated in the vasorelaxation of MVO; 3) MVO-suppressed  $Ca^{2+}$  influx in rat mesenteric arteries rings contributed to the vasorelaxation effects of MVO; and 4) the release of  $Ca^{2+}$  or  $\beta_2$ -adrenoceptors had little effect on the vasorelaxation of MVO. Our results firstly revealed that the underlying mechanisms of MVO-induced vasorelaxation were multiple for the first time *via* the combined application of network pharmacology and experiment, which directly pointed out the research direction and obtained reliable results (Wang et al., 2019; Jiang et al., 2021). Indeed, as previously noted, the two types of investigation have limitations. Therefore, a combination of the two types should be applied so that both of them can make up for each other's shortcomings. Actually, the combined approach found the active compounds and activity mechanisms quickly and achieved the change from experience-based medicine to evidence-based medicine (Zhou et al., 2020), which supplied novel guidance, strategy, thinking, and research for TCM. Nevertheless, our data did not yet allow us to know what behaviors of MVO were *in vivo* and whether MVO protected the hypertension-related vascular dysfunction and other complications. Hence, *in vivo* experiments should be performed to study the underlying mechanism of MVO-induced vasorelaxation for further investigation.

## 6 CONCLUSION

In the present study, the results of GC-MS revealed that 29 compounds were found in MVO and  $\alpha$ -,  $\beta$ -, and  $\gamma$ -eudesmol occupied a large proportion in MVO. The network pharmacology indicated that a total of seven ingredients, of which the top three were beta-caryophyllene, palmitic acid, and (+)- $\beta$ -selinene, were more likely to show therapeutic effects against hypertension *via* multiple targets and multi-pathways. Moreover, the results highlighted the idea that MVO could regulate the expression levels of targets, especially for TNF, CHRM1, ACE, IL10, PTGS2, REN, and F2, as well as neuroactive ligand-receptor interaction, the calcium signaling pathway, and PI3K-Akt signaling pathway to treat hypertension. Similarly, the vasorelaxant effects and mechanisms of MVO were identified in aortic rings, mainly including the PI3K-Akt-NO pathway,  $K_V$  pathway as well as

$Ca^{2+}$  channel. The present study not only reported the vasorelaxant activity and the underlying mechanisms of MVO but also provided a useful strategy for TCM because of the combination of network pharmacology and experiments *in vitro*.

## DATA AVAILABILITY STATEMENT

The original contributions presented in the study are included in the article/**Supplementary Material**, further inquiries can be directed to the corresponding authors.

## ETHICS STATEMENT

The animal study was reviewed and approved by Animal Management Rules of the Ministry of Health of China.

## AUTHOR CONTRIBUTIONS

J-FX contributed to the drafting of the manuscript. HA and CP obtained funding, designed, conceived and supervised process, and revised the manuscript. Others were involved in searching, screening the search results, translation, and data collection. All the authors have read and approved the final manuscript.

## FUNDING

This work was supported by the Program of the National Natural Science Foundation of China (81503272 and 81630101), the Application Foundation Research Project of Sichuan Provincial Department of Science and Technology (2017JY0187), and the Xinglin Scholar Research Promotion Project of Chengdu University of TCM (2018016).

## SUPPLEMENTARY MATERIAL

The Supplementary Material for this article can be found online at: <https://www.frontiersin.org/articles/10.3389/fphar.2022.812716/full#supplementary-material>

## REFERENCES

- Akhtar, A. M., Al, D., and Eid, A. H. (2016). Anti-hypertensive Herbs and Their Mechanisms of Action: Part I. *Front. Pharmacol.* 7 (50), 50. doi:10.3389/fphar.2016.00050
- Anfinogenova, Y. J., Baskakov, M. B., Kovalev, I. V., Kilin, A. A., Dulin, N. O., and Orlov, S. N. (2004). Cell-volume-dependent Vascular Smooth Muscle Contraction: Role of  $Na^+$ ,  $K^+$ ,  $2Cl^-$  Cotransport, Intracellular  $Cl^-$  and L-type  $Ca^{2+}$  Channels. *Pflugers Arch.* 449 (1), 42–55. doi:10.1007/s00424-004-1316-z
- August, P. (2004). Overview: Mechanisms of Hypertension: Cells, Hormones, and the Kidney. *J. Am. Soc. Nephrol.* 15 (8), 1971–1973. doi:10.1097/01.ASN.0000133197.23478.76
- Baek, Y. J. (2004). *Influence of  $\beta$ -eudesmol on Blood Pressure and Aortic Strips Contractility of the Rat*. Gwangju Metropolitan City, South Korea: Chosun University.
- Basha, R. H., and Sankaranarayanan, C. (2016).  $\beta$ -Caryophyllene, a Natural Sesquiterpene Lactone Attenuates Hyperglycemia Mediated Oxidative and Inflammatory Stress in Experimental Diabetic Rats. *Chem. Biol. Interact.* 245 (245), 50–58. doi:10.1016/j.cbi.2015.12.019
- Beaney, T., Schutte, A. E., Stergiou, G. S., Borghi, C., Burger, D., Charchar, F., et al. (2020). May Measurement Month 2019: The Global Blood Pressure Screening Campaign of the International Society of Hypertension. *Hypertension* 76 (2), 333–341. doi:10.1161/hypertensionaha.120.14874
- Chen, C. R., Tan, R., Qu, W. M., Wu, Z., Wang, Y., Urade, Y., et al. (2011). Magnolol, a Major Bioactive Constituent of the Bark of *Magnolia officinalis*,

- Exerts Antiepileptic Effects via the GABA/benzodiazepine Receptor Complex in Mice. *Br. J. Pharmacol.* 164 (5), 1534–1546. doi:10.1111/j.1476-5381.2011.01456.x
- Chen, Z., Lin, T., Liao, X., Li, Z., Lin, R., Qi, X., et al. (2021). Network Pharmacology Based Research into the Effect and Mechanism of Yinchenhao Decoction against Cholangiocarcinoma. *Chin. Med.* 16 (1), 13. doi:10.1186/s13020-021-00423-4
- Davis, J. R., Giardina, J. B., Green, G. M., Alexander, B. T., Granger, J. P., and Khalil, R. A. (2002). Reduced Endothelial NO-cGMP Vascular Relaxation Pathway during TNF-Alpha-Induced Hypertension in Pregnant Rats. *Am. J. Physiol. Regul. Integr. Comp. Physiol.* 282 (2), R390–R399. doi:10.1152/ajpregu.00270.2001
- Di, B., Xu, X., and Chen, X. (2020). The Correlation of Cytokines IL-10 and IL-17 with Blood Pressure and Immune Level in Patients with Essential Hypertension. *Acta Med. Mediterranea* 36 (3), 1421–1425. doi:10.19193/0393-6384\_2020\_3\_221
- Eichhorn, B., and Dobrev, D. (2007). Vascular Large Conductance Calcium-Activated Potassium Channels: Functional Role and Therapeutic Potential. *Naunyn Schmiedebergs Arch. Pharmacol.* 376 (3), 145–155. doi:10.1007/s00210-007-0193-3
- Fang, X. P., Lu, Y. S., Wu, Q., and Hu, G. P. (2012). Comparative Research on Volatile Oil Components of Magnolia officinalis in Guizhou Different Regions. *Chin. J. Exp. Traditional Med. Formulae* 18 (17), 142–145. doi:10.13422/j.cnki.syfxj.2012.17.064
- Ferreira, H. C., Serra, C. P., Lemos, V. S., Braga, F. C., and Cortes, S. F. (2007). Nitric Oxide-dependent Vasodilatation by Ethanolic Extract of Hancornia Speciosa via Phosphatidyl-Inositol 3-kinase. *J. Ethnopharmacol.* 109 (1), 161–164. doi:10.1016/j.jep.2006.06.009
- Fountain, S. J., Cheong, A., Flemming, R., Mair, L., Sivaprasadarao, A., and Beech, D. J. (2004). Functional Up-Regulation of KCNA Gene Family Expression in Murine Mesenteric Resistance Artery Smooth Muscle. *J. Physiol.* 556 (Pt 1), 29–42. doi:10.1111/jphysiol.2003.058594
- Fujita, T. (2014). Mechanism of Salt-Sensitive Hypertension: Focus on Adrenal and Sympathetic Nervous Systems. *J. Am. Soc. Nephrol.* 25 (6), 1148–1155. doi:10.1681/ASN.2013121258
- Ganitkevich, V., and Isenberg, G. (1990). Isolated guinea Pig Coronary Smooth Muscle Cells. Acetylcholine Induces Hyperpolarization Due to Sarcoplasmic Reticulum Calcium Release Activating Potassium Channels. *Circ. Res.* 67 (2), 525–528. doi:10.1161/01.res.67.2.525
- Gao, Y., Portugal, A. D., Negash, S., Zhou, W., Longo, L. D., and Usha Raj, J. (2007). Role of Rho Kinases in PKG-Mediated Relaxation of Pulmonary Arteries of Fetal Lambs Exposed to Chronic High Altitude Hypoxia. *Am. J. Physiol. Lung Cell Mol Physiol* 292 (3), L678–L684. doi:10.1152/ajplung.00178.2006
- Gomolak, J. R., and Didion, S. P. (2014). A Role for Innate Immunity in the Development of Hypertension. *Med. Hypotheses* 83 (6), 640–643. doi:10.1016/j.mehy.2013.12.027
- Han, H., Jung, J. K., Han, S. B., Nam, S. Y., Oh, K. W., and Hong, J. T. (2011). Anxiolytic-like Effects of 4-O-Methylhonokiol Isolated from Magnolia officinalis through Enhancement of GABAergic Transmission and Chloride Influx. *J. Med. Food* 14 (7-8), 724–731. doi:10.1089/jmf.2010.1111
- Hao, H. F., Liu, L. M., Pan, C. S., Wang, C. S., Gao, Y. S., Fan, J. Y., et al. (2017). Rhynchophylline Ameliorates Endothelial Dysfunction via Src-PI3K/Akt-eNOS Cascade in the Cultured Intrarenal Arteries of Spontaneous Hypertensive Rats. *Front. Physiol.* 8, 928. doi:10.3389/fphys.2017.00928
- He, X. Z., Jiang, J. H., Xu, X. N., and Peng, X. (2012). Analysis of the Essential Oil of Cortex Magnolia officinalis by GC-MS. *Appl. Chem. Industry* 41 (02), 352–357+359. doi:10.16581/j.cnki.issn1671-3206.2012.02.003
- He, D., Zhang, Z.-y., Huang, J.-h., Du, Q., Peng, W.-j., Yu, R., et al. (2019). A Network Pharmacology-Based Strategy for Predicting Active Ingredients and Potential Targets of LiuWei DiHuang Pill in Treating Type 2 Diabetes Mellitus. *Drug Des. Dev. Ther.* 13, 3989–4005. doi:10.2147/dddt.s216644
- Huang, Y., and Kwok, K. H. (1998). Beta-adrenoceptor-mediated Relaxation Inhibited by Tetrapentylammonium Ions in Rat Mesenteric Artery. *Life Sci.* 62 (2), PL19–25. doi:10.1016/s0024-3205(97)01065-5
- Jiang, N., Li, H., Sun, Y., Zeng, J., Yang, F., Kantawong, F., et al. (2021). Network Pharmacology and Pharmacological Evaluation Reveals the Mechanism of the Sanguisorba officinalis in Suppressing Hepatocellular Carcinoma. *Front. Pharmacol.* 12, 618522. doi:10.3389/fphar.2021.618522
- Jiye Chen, J., Zhang, Y., Wang, Y., Jiang, P., Zhou, G., Li, Z., et al. (2021). Potential Mechanisms of Guizhi Decoction against Hypertension Based on Network Pharmacology and Dahl Salt-Sensitive Rat Model. *Chin. Med.* 27 (161), 34. doi:10.1186/s13020-021-00446-x
- Kaneda, T., Sasaki, N., Urakawa, N., and Shimizu, K. (2016). Endothelium-Dependent and -Independent Vasodilator Effects of Dimethyl Sulfoxide in Rat Aorta. *Pharmacology* 97 (3-4), 171–176. doi:10.1159/000443894
- Kelm, M. A., and Nair, M. G. (2000). A Brief Summary of Biologically Active Compounds from Magnolia Spp. *Stud. Nat. Prod. Chem.* 24 (00), 845–873. doi:10.1016/s1572-5995(00)80056-3
- Kidoguchi, S., Sugano, N., Tokudome, G., Yokoo, T., Yano, Y., Hatake, K., et al. (2021). New Concept of Onco-Hypertension and Future Perspectives. *Hypertension* 77 (1), 16–27. doi:10.1161/HYPERTENSIONAHA.120.16044
- Kizhakekuttu, T. J., and Widlansky, M. E. (2010). Natural Antioxidants and Hypertension: Promise and Challenges. *Cardiovasc. Ther.* 28 (4), e20–32. doi:10.1111/j.1755-5922.2010.00137.x
- Kume, H., and Kotlikoff, M. I. (1991). Muscarinic Inhibition of Single KCa Channels in Smooth Muscle Cells by a Pertussis-Sensitive G Protein. *Am. J. Physiol.* 261 (6 Pt 1), C1204–C1209. doi:10.1152/ajpcell.1991.261.6.C1204
- Lee, C. H., Poburko, D., Sahota, P., Sandhu, J., Ruehlmann, D. O., and van Breemen, C. (2010). The Mechanism of Phenylephrine-Mediated [Ca(2+)](i) Oscillations Underlying Tonic Contraction in the Rabbit Inferior Vena Cava. *J. Physiol.* 534 (Pt 3), 641–650. doi:10.1111/j.1469-7793.2001.t01-1-00641.x
- Lee, Y. J., Choi, D. Y., Han, S. B., Kim, Y. H., Kim, K. H., Seong, Y. H., et al. (2012). A Comparison between Extract Products of Magnolia officinalis on Memory Impairment and Amyloidogenesis in a Transgenic Mouse Model of Alzheimer's Disease. *Biomol. Ther. (Seoul)* 20 (3), 332–339. doi:10.4062/biomolther.2012.20.3.332
- Lee, J. H., Parveen, A., Do, M. H., Lim, Y., Shim, S. H., and Kim, S. Y. (2018). Lespedeza Cuneata Protects the Endothelial Dysfunction via eNOS Phosphorylation of PI3K/Akt Signaling Pathway in HUVECs. *Phytomedicine* 48, 1–9. doi:10.1016/j.phymed.2018.05.005
- Li, S. (2016). Exploring Traditional Chinese Medicine by a Novel Therapeutic Concept of Network Target. *Chin. J. Integr. Med.* 22 (9), 647–652. doi:10.1007/s11655-016-2499-9
- Lim, D.-Y., and Kee, Y.-W. (2005). Influence of  $\beta$ -eudesmol on Blood Pressure. *Nat. Product. Sci.* 11, 33–40.
- Lou, F. M., Li, Q. F., and Qiu, W. W. (2011). Analysis on the essential oil of Magnolia officinalis Red.et Wils.in Five Different Habitats by GC-MS. *J. Anhui Agri. Sci.* 39 (07), 3934–3937. doi:10.13989/j.cnki.0517-6611.2011.07.083
- Luo, T. T., Lu, Y., Yan, S. K., Xiao, X., Rong, X. L., and Guo, J. (2020). Network Pharmacology in Research of Chinese Medicine Formula: Methodology, Application and Prospective. *Chin. J. Integr. Med.* 26 (1), 72–80. doi:10.1007/s11655-019-3064-0
- Machado, K. D. C., Islam, M. T., Ali, E. S., Rouf, R., Uddin, S. J., Dev, S., et al. (2018). A Systematic Review on the Neuroprotective Perspectives of Beta-Caryophyllene. *Phytother Res.* 32 (12), 2376–2388. doi:10.1002/ptr.6199
- Maranta, F., Spoladore, R., and Fragasso, G. (2017). Pathophysiological Mechanisms and Correlates of Therapeutic Pharmacological Interventions in Essential Arterial Hypertension. *Adv. Exp. Med. Biol.* 956, 37–59. doi:10.1007/5584\_2016\_169
- Murthy, K. S., and Makhlof, G. M. (1997). Differential Coupling of Muscarinic M2 and M3 Receptors to Adenylyl Cyclases V/VI in Smooth Muscle. Concurrent M2-Mediated Inhibition via Galphai3 and M3-Mediated Stimulation via Gbetagamma. *J. Biol. Chem.* 272 (34), 21317–21324. doi:10.1074/jbc.272.34.21317
- Obara, Y., Aoki, T., Kusano, M., and Ohizumi, Y. (2002). Beta-eudesmol Induces Neurite Outgrowth in Rat Pheochromocytoma Cells Accompanied by an Activation of Mitogen-Activated Protein Kinase. *J. Pharmacol. Exp. Ther.* 301 (3), 803–811. doi:10.1124/jpet.301.3.803
- Ohbuchi, T., Haam, J., and Tasker, J. G. (2015). Regulation of Neuronal Activity in Hypothalamic Vasopressin Neurons. *Interdiscip. Inf. Sci.* 21 (3), 225–234. doi:10.4036/iis.2015.B.07
- Otterdal, K., Andreassen, A. K., Yndestad, A., Oie, E., Sandberg, W. J., Dahl, C. P., et al. (2008). Raised LIGHT Levels in Pulmonary Arterial Hypertension:

- Potential Role in Thrombus Formation. *Am. J. Respir. Crit. Care Med.* 177 (2), 202–207. doi:10.1164/rccm.200703-506OC
- Park, W. S., Ko, J. H., Ko, E. A., Son, Y. K., Hong, D. H., Jung, I. D., et al. (2010). The Guanylyl Cyclase Activator YC-1 Directly Inhibits the Voltage-dependent K<sup>+</sup> Channels in Rabbit Coronary Arterial Smooth Muscle Cells. *J. Pharmacol. Sci.* 112 (1), 64–72. doi:10.1254/jphs.09228fp
- Peixoto, P., Aires, R. D., Lemos, V. S., Bissoli, N. S., and Santos, R. L. D. (2017). GPER Agonist Dilates Mesenteric Arteries via PI3K-Akt-eNOS and Potassium Channels in Both Sexes. *Life Sci.* 183, 21–27. doi:10.1016/j.lfs.2017.06.020
- Pérez, G. J., Bonev, A. D., and Nelson, M. T. (2001). Micromolar Ca(2+) from sparks Activates Ca(2+)-Sensitive K(+) Channels in Rat Cerebral Artery Smooth Muscle. *Am. J. Physiol. Cell Physiol.* 281 (6), C1769–C1775. doi:10.1152/ajpcell.2001.281.6.C1769
- Quilley, J., and Qiu, Y. (2005). K(+)-induced Vasodilation in the Rat Kidney Is Dependent on the Endothelium and Activation of K<sup>+</sup> Channels. *Eur. J. Pharmacol.* 508 (1–3), 193–199. doi:10.1016/j.ejphar.2004.12.025
- Scholl, U. I., Stölting, G., Nelson-Williams, C., Vichot, A. A., Choi, M., Loring, E., et al. (2015). Recurrent Gain of Function Mutation in Calcium Channel CACNA1H Causes Early-Onset Hypertension with Primary Aldosteronism. *Elife* 4, e06315. doi:10.7554/eLife.06315
- Sengul, S., Akpolat, T., Erdem, Y., Deric, U., Arici, M., Sindel, S., et al. (2016). Turkish Society of Hypertension and Renal Diseases Changes in Hypertension Prevalence, Awareness, Treatment, and Control Rates in Turkey from 2003 to 2012. *J. Hypertens.* 34 (6), 1208–1217. doi:10.1097/hjh.0000000000000901
- Simon, L. S. (1999). Role and Regulation of Cyclooxygenase-2 during Inflammation. *Am. J. Med.* 106 (5B), 37S–42S. doi:10.1016/s0002-9343(99)00115-1
- Sun, J., Wang, Y., Fu, X., Chen, Y., Wang, D., Li, W., et al. (2015). Magnolia Officinalis Extract Contains Potent Inhibitors against PTP1B and Attenuates Hyperglycemia in Db/db Mice. *Biomed. Res. Int.* 2015, 139451. doi:10.1155/2015/139451
- Tang, F., Liu, M. C., Zhang, S. Y., Wang, J., Sheng, Y. C., Feng, W. W., et al. (2019). Comparative Study on Chemical Composition and Antibacterial Activity of Essential Oils from Patchouli and Magnolia Officinalis Alone and Combination. *Traditional Chin. Drug Res. Clin. Pharmacol.* 30 (04), 478–483.
- Tang, F., Yan, H. L., Wang, L. X., Xu, J. F., Peng, C., Ao, H., et al. (2021). Review of Natural Resources with Vasodilation: Traditional Medicinal Plants, Natural Products, and Their Mechanism and Clinical Efficacy. *Front. Pharmacol.* 12, 627458. doi:10.3389/fphar.2021.627458
- Thorneloe, K. S., and Nelson, M. T. (2005). Ion Channels in Smooth Muscle: Regulators of Intracellular Calcium and Contractility. *Can. J. Physiol. Pharmacol.* 83 (3), 215–242. doi:10.1139/y05-016
- Volpe, M., Gallo, G., and Tocci, G. (2018). Is Early and Fast Blood Pressure Control Important in Hypertension Management? *Int. J. Cardiol.* 254, 328–332. doi:10.1016/j.ijcard.2017.12.026
- Wang, X., Cheang, W. S., Yang, H., Xiao, L., Lai, B., Zhang, M., et al. (2015). Nuciferine Relaxes Rat Mesenteric Arteries through Endothelium-dependent and -independent Mechanisms. *Br. J. Pharmacol.* 172 (23), 5609–5618. doi:10.1111/bph.13021
- Wang, Z., Linghu, K. G., Hu, Y., Zuo, H., Yi, H., Xiong, S. H., et al. (2019). Deciphering the Pharmacological Mechanisms of the Huayu-Qiangshen-Tongbi Formula through Integrating Network Pharmacology and *In Vitro* Pharmacological Investigation. *Front. Pharmacol.* 10, 1065. doi:10.3389/fphar.2019.01065
- Xu, X. N., Tang, Z. H., Liang, Y. Z., Zhang, L. X., Zeng, M. M., and Deng, J. H. (2009). Comparison of the Volatile Constituents of Different Parts of Cortex magnolia Officinalis by GC-MS Combined with Chemometric Resolution Method. *Front. Pharmacol.* 10 (20), 3466–3472. doi:10.1002/jssc.200900378
- Yang, H. B., Shi, L., Zhan, Y. H., Huang, L. Q., Shao, A. J., Li, J., et al. (2007). Chemical Components in Volatile Oil of the Cortex of Magnolia Officinalis Produced in Hubei Enshi. *China J. Chin. Materia Med.* 32, 42–44+48. doi:10.1002/ajmg.a.32880
- Yang, Z. Y., Wei, Y. F., Zhou, Z. H., and Long, F. (2012). Vasorelaxant Effect on Isolated Rabbit Aortic Rings and Chemical Constituents of n-Butanol Fraction from Leaves of Magnolia officinalis Rehd et Wils. *Nat. Product. Res. Dev.* 24 (3), 298–302.
- Yingyao Zhou, Y., Zhou, B., Pache, L., Chang, M., Khodabakhshi, A. H., Tanaseichuk, O., et al. (2019). Metascape Provides a Biologist-Oriented Resource for the Analysis of Systems-Level Datasets. *Nat. Commun.* 10 (1), 1523. doi:10.1038/s41467-019-09234-6
- Youn, U. J., Fatima, N., Chen, Q. C., Chae, S., Hung, T. M., and Min, B. S. (2013). Apoptosis-inducing and Antitumor Activity of Neolignans Isolated from Magnolia Officinalis in HeLa Cancer Cells. *Phytother. Res.* 27 (9), 1419–1422. doi:10.1002/ptr.4893
- Yu, G., and Wang, J. (2016). Exploring Mechanisms of Panax Notoginseng Saponins in Treating Coronary Heart Disease by Integrating Gene Interaction Network and Functional Enrichment Analysis. *Chin. J. Integr. Med.* 22 (8), 589–596. doi:10.1007/s11655-016-2472-7
- Zhang, J. R., Lu, Q. B., Feng, W. B., Wang, H. P., Tang, Z. H., Cheng, H., et al. (2018). Nesfatin-1 Promotes VSMC Migration and Neointimal Hyperplasia by Upregulating Matrix Metalloproteinases and Downregulating PPAR $\gamma$ . *Biomed. Pharmacother.* 102, 711–717. doi:10.1016/j.biopha.2018.03.120
- Zhang, Q., An, R., Tian, X., Yang, M., Li, M., Lou, J., et al. (2017).  $\beta$ -Caryophyllene Pretreatment Alleviates Focal Cerebral Ischemia-Reperfusion Injury by Activating PI3K/Akt Signaling Pathway. *Neurochem. Res.* 42 (5), 1459–1469. doi:10.1007/s11064-017-2202-3
- Zhou, Z. Y., Zhao, W. R., Shi, W. T., Xiao, Y., Ma, Z. L., Xue, J. G., et al. (2019). Endothelial-Dependent and Independent Vascular Relaxation Effect of Tetrahydropalmatine on Rat Aorta. *Front. Pharmacol.* 10, 336. doi:10.3389/fphar.2019.00336
- Zhou, Z., Chen, B., Chen, S., Lin, M., Chen, Y., Jin, S., et al. (2020). Applications of Network Pharmacology in Traditional Chinese Medicine Research. *Evid. Based Complement. Alternat Med.* 2020, 1646905. doi:10.1155/2020/1646905

**Conflict of Interest:** The authors declare that the research was conducted in the absence of any commercial or financial relationships that could be construed as a potential conflict of interest.

**Publisher's Note:** All claims expressed in this article are solely those of the authors and do not necessarily represent those of their affiliated organizations, or those of the publisher, the editors and the reviewers. Any product that may be evaluated in this article, or claim that may be made by its manufacturer, is not guaranteed or endorsed by the publisher.

Copyright © 2022 Xu, Xia, Wan, Yang, Wu, Peng and Ao. This is an open-access article distributed under the terms of the Creative Commons Attribution License (CC BY). The use, distribution or reproduction in other forums is permitted, provided the original author(s) and the copyright owner(s) are credited and that the original publication in this journal is cited, in accordance with accepted academic practice. No use, distribution or reproduction is permitted which does not comply with these terms.